TEMPORAL AND SPATIAL ANALYSIS OF STREAM AND GROUNDWATER INTERACTIONS

By

Ryan Eugene Warden

A thesis

submitted in partial fulfillment

of the requirements for the degree of

Master of Science in Hydrological Sciences

Boise State University

December 2011

BOISE STATE UNIVERSITY GRADUATE COLLEGE

DEFENSE COMMITTEE AND FINAL READING APPROVALS

of the thesis submitted by

Ryan Eugene Warden

Thesis Title: Temporal and Spatial Analysis of Stream and Groundwater Interactions

Date of Final Oral Examination: 22 April 2011

The following individuals read and discussed the thesis submitted by student Ryan Eugene Warden, and they evaluated his presentation and response to questions during the final oral examination. They found that the student passed the final oral examination.

James P. McNamara, Ph.D.	Chair, Supervisory Committee
Shawn G. Benner, Ph.D.	Member, Supervisory Committee
Jennifer Pierce, Ph.D.	Member, Supervisory Committee

The final reading approval of the thesis was granted by James P. McNamara, Ph.D., Chair of the Supervisory Committee. The thesis was approved for the Graduate College by John R. Pelton, Ph.D., Dean of the Graduate College.

ACKNOWLEDGEMENTS

This thesis includes support and work of many more individuals than the title page reflects and would not have been possible without the technical, financial, and emotional support of those individuals. For technical support, direction, and serving as my primary advisor, I would like to thank Dr. James McNamara. Dr. McNamara always had an open door to hear questions, and provide insight into the research questions and methods. I would also like to thank Dr. Shawn Benner and Dr. Jen Pierce for being part of my committee and the numerous faculty members of the Geosciences Department at Boise State University that offered support and direction for this study.

I am thankful for the additional technical assistance by way of field work and instrumentation by graduate students at Boise State University. The list of contributors includes: Brain Anderson, Alden Shallcross, Brian Hanson, Dan Stanaway, and Pam Aishlin. Additional technical assistance was provided by Idaho State University from Dr. Colden Baxter for supplying instruments detrimental to the research.

Funding for the research as well for my studies was largely provided by Boise State University through graduate teaching and research assistantships in the Geosciences Department. Additional funding for this research was provided by a Geological Society of America student grant.

Finally, I would like to thank my wife Ursula for her continual support for my efforts and for consistent encouragement throughout the project. Her support was the foundation for the production of this thesis as well as its completion. Thank you, Ursula, for your gift of unwavering patience and for giving so much of yourself in support of the project. I would also like to thank all my parents, family, and friends for encouragement on this long journey.

ABSTRACT

Water chemistry and ecology of streams are impacted by the amount of water that exchanges between the surface water system and the adjacent saturated area, called the hyporheic zone, a dynamic area of stream channel sediments, which undergoes down-welling or up-welling of stream water. The rate and volume of water exchange between the surface water and the hyporheic zone are primary controls on stream ecology, but are challenging to assess. A common approach is to model the exchange rate with a one-dimensional advection-dispersion equation that includes solute exchange with transient storage zones, which is referred to as a transient storage model. OTIS, a computerized transient storage model, utilizes four hydraulic parameters that represent the stream and the hyporheic zone, which gives a simple measure of the size of the hyporheic zone and its exchange rate with the surface water. This study investigates the influences on hyporheic exchange across temporal and spatial scales to better understand the parameter variability associated with the transient storage model. Thirteen conservative tracer experiments were conducted, which involved multiple tracer injections in the same reach of a small, plane-bed stream in order to determine how seasonal changes affect hyporheic parameters. Another nine alluvial streams were used to conduct more conservative tracer experiments involving two reaches per stream with varying stream channel types but with similar alluvium geology to determine how spatial variations affect the hyporheic parameters. The tracer experiments repeated in the same stream were done across various discharges ranging from 500 to 8 L/s and across different seasons. The other nine

alluvial streams tracer experiments were conducted within the same month with various discharges ranging from 100 to 29.8 L/s. Relationships between the hydraulic parameters and transient storage metrics were compared to discharge, velocity, stream unit power, and Darcy-Weisbach friction factor, which are simple channel descriptors to compare different streams and reaches at different discharge rates. Results show that at a specific reach location, discharge relates linearly to A_s and α, showing that discharge is a major contributor to the hyporheic processes. When comparing the spatially different but similar sites, the correlation of discharge to the hydraulic parameters weakens to a slight correlation, showing that other site-specific processes are occurring at each reach that are influencing the variability of hyporheic processes. Preliminary results show that α may not spatially change across streams that are similar in characterization, although further research needs to be conducted to see if spatially different, but similar streams, result in the same temporal trend of the exchange coefficient, α.

TABLE OF CONTENTS

LIST OF FIGURES

LIST OF TABLES

1. INTRODUCTION

Water chemistry and ecology of streams are impacted by the amount of water that exchanges between the surface water system and the adjacent saturated area, called the hyporheic zone, a dynamic area of stream channel sediments that undergo down-welling or up-welling of stream water. For example, stream water high in dissolved oxygen (DO) can move down into the low DO hyporheic zone and impact the chemical reactions that occur with the mixing of this water, thus influencing the water chemistry, stream ecology, and water quality. Therefore, it is important to understand the physical controls that facilitate these interactions, especially its variability from temporal and spatial changes.

The rate and volume of water exchange between surface water and the hyporheic zone are primary controls on stream ecology, but are challenging to assess. A common approach is to model the exchange rate with a one-dimensional advection-dispersion equation that includes solute exchange with transient storage zones and is commonly referred to as a transient storage model. The One-Dimensional Transport with Inflow and Storage model (OTIS) is widely used to characterize the stream and the hyporheic zone by using a computerized transient storage model equation (Runkel, 1998) (See Section 1.1, Scientific Background, Modeling-Parameterization). OTIS utilizes breakthrough curves derived from stream tracer experiments. In stream tracer experiments, a solute is added to the stream and concentrations of the solute are measured over time. The solute will undergo the same processes that the stream water goes through and thus the concentration of the solute will reflect the processes of that stream, specifically the hyporheic processes. The measured concentrations create breakthrough curves that have the streams characteristics imprinted on it by the timing and the concentration of the solute. Simple models that only represent the advection and dispersion processes in a stream fail to account for a delay of the rising concentration or the persistence of the tail in the breakthrough curves (Bencala & Walters, 1983). It is in the shoulder of the rising edge and the persistence of the tail that are the essential features that are modeled in OTIS that result in parameterization of the hyporheic zone.

OTIS utilizes four parameters that represent the stream and the hyporheic zone, which are: the cross-sectional area of the main stream channel, A; storage zone, A_s; dispersion coefficient, D; and, the storage zone exchange coefficient, α. These hydraulic parameters give a simple measure for the size of the hyporheic zone and its exchange rate; however, numerous studies have shown that these parameters vary with different streams and vary from seasonal changes (D'Angelo et al., 1993; Hart et al., 1999; Harvey et al., 2003; Jin & Ward, 2005; Zarnetske et al., 2007; Stofleth et al., 2008). An appropriate interpretation of the meaning of the OTIS parameters relies on understanding the relationships between those parameters and the stream properties. For example, Zarnetske et al. (2007) showed that discharge, Q, is a primary factor influencing and controlling the hydraulic parameters of the stream and hyporheic zone. If discharge is primarily the controlling or influencing factor on hyporheic exchange in a stream, then one would expect to see this not only in repeat experiments in the same stream but also in other streams.

Due to the popularity of OTIS, and the associated parameters, for characterizing flow in hyporheic zones, it is essential to understand if parameter variability is a function of spatial changes in properties that promote hyporheic exchange, temporal changes in stream hydraulics, or simply mathematical artifacts of the modeling process. This study investigates the influences on hyporheic exchange across temporal and spatial changes to better understand the parameter variability involved with the transient storage model. Specifically, this project tests the hypothesis that discharge is a primary control on the OTIS parameters that are commonly used to described hyporheic exchange. The following questions were formed from the research hypothesis: how do hydraulic parameters vary in time with relationship to discharge, velocity, channel friction factor, and stream unit power? Can these relationships be extended to spatially similar streams, or in other words, can temporal relationships relate hydraulic parameters of different streams? Further, this research investigates if the OTIS parameters are valuable metrics of stream characterization.

Stream tracer experiments using rhodamine WT were conducted in the Dry Creek Experimental Watershed (DCEW) at a range of discharges to assess temporal variability, and in nine other streams at similar discharges to assess spatial variability. The resulting breakthrough curves from the stream tracer experiments were then modeled with OTIS. Correlations were sought between the OTIS parameters and various stream characteristics in order to understand the sources of variability of the optimal OTIS parameters.

1.1 Scientific Background

A conceptual model can be used to better understand the hyporheic exchange by imagining a stream as a pipe that transports catchment water down-slope. Attached to the pipe are several small boxes that can store water and then reintroduce that water back into the pipe. These small boxes are representative of the hyporheic sediments that receive stream water and then allow it to flow back into the main stream. When this occurs, the water that returns to the stream can be chemically different than when it entered the sediments. The boxes used in the conceptual model, the hyporheic zone, are an integral part of the catchment and can change the quality and chemistry of the water.

White (1993) offered a definition of the hyporheic zone that separates it from the groundwater zone and the surface water zone. The concept is that the hyporheic zone is the area that is saturated beneath and lateral to the stream that has portions of stream water within it. This differentiates the groundwater zone from the hyporheic zone because the groundwater zone is not influenced by stream water.

Hyporheic exchange can occur at many different scales, as small as centimeters to meters, ranging up to large scales that involve regions or catchments of 100's of meters to a couple kilometers. Mallard et al. (2002) proposed a perspective of how to visualize the complexity of hyporheic exchange by seeing the surface and subsurface exchange of water as a three-dimensional mosaic that occurs over several different spatial scales. This spatial variation for exchanging water brings up several problems for figuring out how water flows through the sediments and how influential each flow path is towards the chemistry, biology, and any related characteristic to the stream. The current debate among researchers is which scale is most important to hyporheic exchange (Boulton et al., 1998).

The impact of the hyporheic exchange on surface water can be broken down into the different scales that are most affected. Boulton et al. (1998) proposed that the functional significance of the hyporheic zone depends on its flux and connection with the stream across all possible scales. This can be understood by looking at the scale of interest to see the amount of surface water being exchanged and then assessing the impact of the exchanged water to get an idea of its significance. For example, a micro-organism will mainly be affected by small scale exchanges in the range of centimeters, whereas the concentration of certain nutrients or chemicals at a downstream location will be impacted by a reach or catchment scale ranging from meters to kilometers, although the main impact to the stream will be dictated by how much exchange actually occurs on each scale of interest. Stream ecologists have long recognized the importance of hyporheic zones on streams (Hynes, 1975) due to the influence on zoobenthic habitat and fish reproduction (Valett et al., 1990).

Findlay (1995) found that hyporheic exchange had potential to cause significant changes in the stream water chemistry by allowing biogeochemical processes to occur due to the down-welling of the stream water into the active sediment. Up-welling areas of the hyporheic zone can provide nutrients into the stream from the nutrient rich groundwater, just as the down-welling water can provide oxygen for organisms living within the sediments (Boulton et al., 1998, Valett et al., 1990). Looking at dissolved organic carbon, DOC, it was found that approximately 50% of the DOC in the stream water was utilized by micro-organisms when it exchanged with the sediments (Findlay et al., 1993). Baxter and Hauer (2000) found that bull trout used up-welling areas in the streambed for spawning and that the bull trout redds are usually located in down-welling areas. Stream ecology is strongly influenced by where and how the hyporheic exchange occurs in the stream and can provide a vital habitat. Nutrients and oxygen are not the only thing that can be altered by the hyporheic zone. Water temperature within the hyporheic zone can be different than the surface temperature and thus provide a flux of temperatures entering and exiting the stream sediments (White et al., 1987).

When looking at the chemistry of the water as it enters the hyporheic sediments, a set of complex reactions can occur, affecting nutrients and chemicals. Once the oxygen is used up, other reactions start to occur, using nutrients like nitrogen (Mallard et al., 2002). The hyporheic zone may allow concentrations to rise or fall depending on the exchange and the residence time within the hyporheic zone, which will dictate how many chemical processes can occur (Morrice et al., 1997). Water chemistry and the concentration of nutrients found in the stream can be a function of the hyporheic zone and its exchange with the stream water, making an important impact on the stream ecosystem.

As previously discussed, hyporheic exchange is characterized as the down-welling of surface water into the sediments of the hyporheic zone and then up-welling of that water back into the stream. Hyporheic exchange therefore can occur many times in a stream reach going back and forth through the sediments in different flow paths and with different resident times. Those flow paths in the hyporheic zone could be in and out of the bottom of a streambed where slope breaks occur or could be through a stream bank on an inside corner of a meandering bend.

Hyporheic exchange can follow Darcy's law when the flow paths are laminar saturated flow through the sediment medium. Darcy's Law requires a gradient and a porous medium in order to have flow where the gradient for hyporheic exchange can be provided by many different mechanisms such as topography of the streambed (Harvey &

Bencala, 1993). The study done by Harvey and Bencala (1993) found that topography enhanced the exchange between the stream and sediments and thus could have important consequences for solute transport, retention, and transport of nutrients in a basin. Anderson et al. (2005) used stream morphologic features to see the influence on hyporheic exchange. They found that the size and spacing of channel-unit-scale morphologic features and concavity in the surface profile provided sufficient influence to be able to model its characteristics. Related to this topography as an influence to hyporheic exchange is the idea that a stream's bedform and its amplitude will also sway the exchange (Tonina & Buffington, 2007). Tonina and Buffington (2007) illustrated this using a laboratory plume to indicate that the bedform of a stream can be a major mechanism to induce exchange at certain discharges. Buffington and Tonina (2009) went further into the idea of channel morphology influencing and controlling the mechanics of hyporheic exchange, by describing different channel types, their associated flow paths, and exchanges that would influence the hyporheic zone.

The second part of Darcy's law, a porous medium, refers to the type of sediments that the water is flowing through that dictate the amount of exchange that can occur. Morrice et al. (1997) looked at different geological compositions in streams and assessed that alluvial characteristics influence hyporheic exchange. Results showed that alluvial characteristics, such as clays, sands, and gravels in varying amounts will strongly influence the hyporheic exchange rate. The alluvium characteristics are key controlling factors of the hyporheic exchange because they relate directly to the hydraulic conductivity of the sediments (Storey et al., 2003).

Delineation of the Hyporheic Zone

Delineating and defining the hyporheic zone has evolved through an interdisciplinary perspective. The term hyporheic zone has become known as the area beneath and adjacent to a stream where surface and subsurface water interact within the stream sediments and many different ways have been derived in order to delineate this hyporheic zone (White, 1993).

Early researchers identified organisms in the streambed that were associated with the hyporheic zone to determine its extent (Hynes, 1974). This biology perspective of distributions of hypogean (groundwater) and epigaean (channel) invertebrates was attempted to distinguish the boundary of the hyporheic zone (White, 1993). White et al. (1987) used temperature changes in the sediment as a way of determining the presence and extent of the hyporheic zone. Triska et al. (1989) used an injected conservative solute to see the extent that it would spread into the sediments. They defined the hyporheic zone as the area that received 10% of the stream water as its source and also used chemical gradients to identify biologically active hyporheic zones within the sediment.

Hydrologists took the approach of identifying the hyporheic zone by determining the flow paths of the exchanging water. The distribution of the hyporheic zones have been described as “functions of channel water hydraulics, or combinations of channel water and groundwater hydraulics, which determine advective patterns” (White, 1993). White et al. (1987) showed that streambed temperature could be used to determine where the hyporheic zone exists along with its extent in the stream by using a temperature probe that was pushed into the sediments. It showed that a temperature gradient within the sediment existed and was probably the product of down-welling and up-welling stream and groundwater.

Mathematical transient storage equations were developed to describe the transport dynamics in terms that relate to the physical and hydraulic characteristics of the hyporheic zone and streams (Bencala and Walters, 1983). The transient storage equations are modified advection-dispersion equations that are used to parameterize the stream and hyporheic zone through curve fitting solute tracer data, thus giving a measure of the hyporheic zone and its exchange. Triska et al. (1989) injected solute tracers into the stream channel to delineate the hyporheic zone based on the extent that the solute traveled in the lateral sediments of the stream. It was found that the conservative tracer reached 10 meters perpendicular to the stream and stream water contributed about 47% to that area (Triska el al., 1989). Utilizing sub-surface head gradients in the sediments can show movement and flow paths that are involved in the hyporheic zone (Harvey and Bencala, 1993). This method uses piezometers to measure vertical head gradients to understand the flow patterns of the hyporheic zone and can identify areas that are up-welling or down-welling in the stream. Many uncertainties can arise with this method due to the complexity of the head distribution, need for lots of instrumentation, and the influence of changes in hydraulic conductivity (Harvey & Wagner, 2000).

Complications of delineating the hyporheic zone arise from the variability of the stream. Streams and their ecosystems are dynamic and change according to environmental input and outputs. Changes in discharge, temperature, sediment load, groundwater gradients, and riparian areas can change the hyporheic exchange and its extent, thus the hyporheic zone is variable on a temporal and spatial scale.

<u>Modeling-Parameterization</u>

Research done by Bencala and Walters (1983) noted that stream tracer experiments could be used to simulate solute transport through “dead zones,” temporary storage areas, in a mountainous stream, which could relate to the hyporheic exchange in that stream. These stream tracer experiments involve adding a solute, conservative or non-conservative in regards to reactions in the stream and the streambed, and measuring the concentrations of the solute in time at stations downstream from the injection point. The idea of adding a solute to the stream and measuring the concentrations is that the solute will undergo the same mechanisms that the stream water does and thus the concentration of the solute should reflect the mechanism of the stream. The gathered data creates a breakthrough curve that has the streams characteristics imprinted on it by the timing and the concentration of the solute at the measuring point.

The breakthrough curves are used in a one-dimensional advection-dispersion analysis to study the transport in streams. Simple models that only represent the advection and dispersion processes in a stream fail to account for a delay or ‘tail’ in the breakthrough curves (Bencala & Walters, 1983). Figure 1.1 shows a representation of breakthrough curves where certain processes are considered. Figure 1.1a solely shows what would occur if advection was the only process involved on the solute. Figure 1.1b and 1.1c add more processes onto the breakthrough curves to represent how the curves change with more mechanisms. Figure 1.1c is a standard representation of a breakthrough curve collected from a stream where the simple advection-dispersion model fails to explain the pronounce curves, which Bencala and Walters (1983) explained by adding a term for “dead zones” or temporary storage.

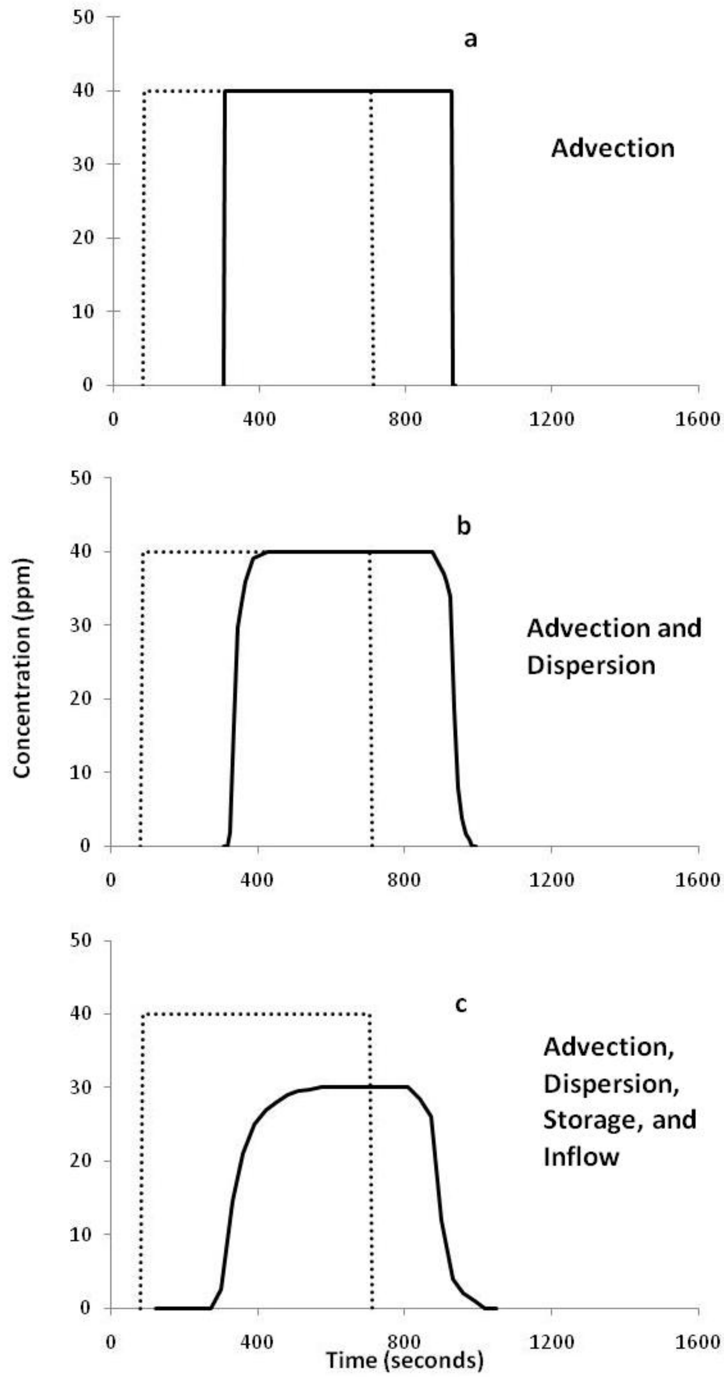

Figure 1.1. Illustration of Breakthrough Curves and processes influencing them. Dotted line is the concentration at the injection point and the dark line is the measured concentration downstream. (Modified from D'Angelo et al., 1993).

The model equation that incorporates advection, dispersion, and terms for storage is referred to as the Transient Storage Model and is defined by Bencala and Walters (1983) as

$$\frac{\partial C}{\partial t} = -\frac{Q}{A}\frac{\partial C}{\partial x} + \frac{1}{A}\frac{\partial}{\partial x}\left(AD\frac{\partial C}{\partial x}\right) + \frac{qLIN}{A}\left(C_L - C\right) + \propto \left(C_S - C\right) \tag{1.1}$$

$$\frac{\partial C_S}{\partial t} = \propto \frac{A}{A_S}\left(C - C_S\right) \tag{1.2}$$

Where

C solute concentration in the stream, mg l^{-1}

Q volumetric flow rate, m^2 s^{-1}

A cross-sectional area of the channel, m^2

D dispersion coefficient, m^2 s^{-1}

qLIN lateral volumetric inflow rate (per length), m^3 s^{-1} m^{-1}

C_L solute concentration in lateral inflow, mg^3 l^{-1}

C_S solute concentration in the storage zone, m^2

A_S cross-sectional area of the storage zone, m^2

α stream storage exchange coefficient, s^{-1}

t time, s

x distance, m

The primary assumptions with this model are that solute concentration varies only in the longitudinal direction, and that the transient storage can be described by an exponential distribution (Bencala & Walters, 1983). Several other assumptions can be made along with the primary assumptions as presented by Runkel (1998). Stream channel assumptions are:

- The processes affecting solute concentrations, the breakthrough curves, include advection, dispersion, lateral inflow, lateral outflow, and transient storage.
- The model parameters describing all processes can be spatially variable.
- The model parameters for advection and lateral inflow may be temporally variable. The parameters that can temporally vary are the volumetric flow rate, main channel cross-sectional area, lateral inflow rate, and the solute concentration associated with lateral inflow.

The storage zone assumptions are:

- Advection, dispersion, lateral inflow, and lateral outflow do not occur in the storage zone. Transient storage is the only physical process affecting solute concentrations.
- All model parameters describing transient storage can be spatially variable.
- All model parameters describing transient storage are temporally constant.

Although the transient storage model represents the processes occurring in streams, Bencala and Walters (1983) strictly stated that this “dead zone model” doesn’t physically describe the processes occurring but rather empirically simulates it using the above equations.

Figure 1.2 is presented below to show how theoretically the parameters influence the breakthrough curves. The dispersion affects the first rising curve and the first falling curve, whereas the exchange coefficient affects the immediate second rising curve and the immediate second falling curve. The cross-sectional area of the storage zone affects the tail end of the second rising curve and the tail end of the second falling curve, where the cross-sectional area of the main channel affects the main portion of the rising and falling limbs of the breakthrough curves. This theoretically shows how each of the parameters will be derived from a breakthrough curve as presented by the Stream Solute Workshop (1990).

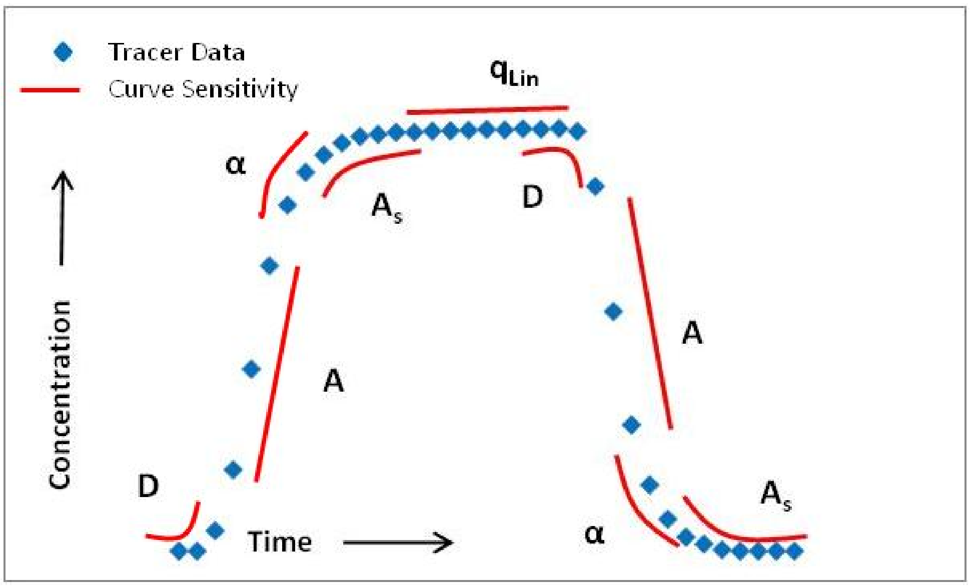

Figure 1.2. Illustration of theoretical parameter sensitivity on a breakthrough curve (modified from Harvey & Wagner, 2000).

The theoretical illustration of Figure 1.2 shows how stream tracer data is modeled resulting in estimates of Q, A, D, α, and A_s. The modeling process starts with using estimates of the parameters to try and get a visual best fit of a modeled tracer curve compared to the actual tracer data. This process of finding a visual best fit is done by trial and error for the estimates of the parameters. The trial and error method can be overwhelming if one tries to tweak all the parameters to get a visual best fit, so it is best to only tweak one parameter at a time. It also helps to do certain parameters first that can give very good initial estimates of the parameters. It is recommended to start with Q, discharge, then move to A, stream cross-sectional area, then D, dispersion, and then work on α, exchange coefficient, and A_s, storage cross-sectional area.

Discharge, Q, can be simply estimated by a mass-balance for a conservative tracer by:

$$C_bQ + C_IQ_I = C_pQ \tag{1.3}$$

Where C is the concentration and the subscripts stand for background, b, plateau, p, and injection solution, I. If the estimated Q is too large or too small, the modeled curve will not match the plateau concentration by being a lower concentration with a too large Q and a higher concentration with a too small Q. Once a good estimate of Q has been found, matching the plateau concentrations, the next parameters can then be estimated.

Parameter A, stream cross-sectional area, can be measured from the field by measuring several cross-section areas of the study stream to find an average cross-section area for an initial estimate for the model. If the estimated A is too small of an estimate or too large, the timing of the plateau event occurs early or later than the observed data, respectively. Once a good fit of A has been found, trial and error comparisons can start for D, dispersion. When good estimates of Q, A, and D are found, the modeling results would resemble something close the solid line curve in Figure 1.1b.

The modeled curve will likely not be a great fit to the tracer data because it does not incorporate transient storage, which affects the shoulder of the rising edge and the persistence of the tail on the tracer data. These are the essential features showing that transient storage is present in the tracer data and not yet accounted for in the model simulation. Further trial and error estimates for α and A_s are done to get a good visual fit accounting for transient storage. Once a good visual fit has occurred, i.e. the modeled curve fits the observed data, the resulting parameters are estimates for the stream characteristics and for transient storage. This process is referred to as inverse modeling because you start with model predictions and work backwards to find the parameters that fit the known tracer data.

Even though estimates can be made from breakthrough curves through modeling, the breakthrough curves are sensitive to the length of the study reach because the hyporheic imprint on the breakthrough curves can be averaged out in longer reaches (Wagner & Harvey, 1997). Wagner & Harvey showed that uncertainty of the parameters and the experimental Damkohler number, DaI, had a strong correlation. The Damkohler number is calculated by:

$$DaI = \frac{\alpha\left(1+\frac{A}{As}\right)L}{v} \tag{1.4}$$

where L is the study reach length and *v* is the channel velocity.

Wagner and Harvey noted that the lowest amount of uncertainty in the parameters was when the DaI was around 1 and that anything that is much smaller or greater than 1 increases the uncertainty that the parameters are unique. The reasoning for this uncertainty coupled with the stream length is explained if the length of the downstream sampling point is in an area that is already at equilibrium with the exchanging of the hyporheic zones. This would allow a shift in the breakthrough curve that then could be modeled by adjusting the dispersion coefficient just as well as adjusting the exchange parameters (Harvey et al., 1996). This problem would lead to a non-unique situation where the breakthrough curves can be solved by several different pairs of parameters. To ensure that the breakthrough curves and model results are unique, it is best to have a DaI that is around 1. If a study reach is too short, it can result with a DaI<< 1; or, if the study reach is too long, then the Dai>> 1, which would increase the uncertainty of the storage zone parameters (Harvey & Wagner, 2000). Wagner and Harvey (1997) suggested that the DaI be between 0.1 and 10 for results to be in an acceptable range where hyporheic exchange will be detectable with breakthrough curves and modeling with the transient storage model.

It is also important to note that the transient storage model is sensitive to only one transient storage area. This transient storage area as presented earlier combines the surface water transient storage and the hyporheic transient storage. Thus, the exchange parameters describe the lumped processes of storage areas of the surface water and hyporheic as well as the exchange of each. Many researchers have criticized the transient storage model for this reason because there is no way to know if the surface water or the hyporheic is contributing more to the parameters. Ensign and Doyle (2005) found that surface water transient storage was a substantial portion of the overall transient storage in streams. Choi et al. (2000) found that a lumped transient storage model, one storage zone model, will reliably characterize a stream and Briggs et al. (2009) found that although a two storage zone model shows more detail on what is going on in the stream a lumped transient storage model characterized the hyporheic characteristics fairly well when compared to the two storage zone model. Therefore, researchers must be careful presenting the model parameters as to account for the uncertainty of hyporheic and surface water processes involved in them.

Parameter Metrics

The four parameters that describe the stream characteristics from the transient storage model are A, D, A_s, and α. The exchange parameters A_s and α cannot be interpreted by themselves to assess the importance of hyporheic exchange in reaches without also considering the other parameters. The exchange parameters are relative to the other parameters and need a way to compare the hyporheic interaction (Lautz et al., 2006). To make these comparisons and understand what the parameters actually mean, several different metrics were derived.

Harvey et al. (1996) presented the storage exchange flux, q_s, the average fluid residence time in the storage, t_s, and the average distance traveled in the channel before entering the storage zone, L_s or uptake length. These metrics are calculated as:

$$q_s = A\alpha \tag{1.5}$$

$$t_s = A_s/q_s \tag{1.6}$$

$$L_s = Q/A\alpha = u/\alpha \tag{1.7}$$

Valett et al. (1996) suggested normalizing A_s so that the magnitude of transient storage could be compared to other streams and/or across different hydrologic conditions. This was done by taking A_s and dividing it by the average cross-section area of the stream channel, A_s/A. This metric is referred as the relative storage size.

Morrice et al. (1997) presented the hydrological retention factor, R_h, which is the storage zone residence time of water per unit of stream reach traveled. R_h is to help compare hydrological retention between streams. Below shows the calculations for it.

$$R_h = t_s/L_s = A_s/Q \qquad (1.8)$$

Runkel (2002) derived a measure of how much a percentage of the median travel time of a solute mass is due to transient storage in a 200 meter reach. This metric is useful because it captures the collective effects of all the parameters in transient storage on the transport of solutes in a stream. To obtain the value for this metric, the transient storage model is ran twice, once with no transient storage and then again with transient storage. Then, it is the difference between the median travel times for the two runs divided by the median travel time with storage. Runkel (2002) presented another way to calculate the metric by using an equation that closely approximates the previous method that still involves the interaction between the advective velocity and transient storage. F_{med} is the fraction of the median travel time due to transient storage and is computed by:

$$F_{med} = (1- e^{-L\alpha/u})\ A_s/\ A+A_s \qquad (1.9)$$

Correlations with the Hydraulic Parameters

The complexity of the hyporheic exchange along with its temporal and spatial variability is the reason to find simple correlations or regression that can explain the behavior of the exchange with the transient storage model. Several researchers have suggested possible relationships for the hydraulic parameters along with the hydraulic metrics.

Simple correlations that have been suggested for the hydraulic parameters and the hydraulic metrics are discharge and velocity, which are likely to be the primary factors for variability (D'Angelo et al., 1993; Hart et al., 1999; Harvey et al., 2003; Jin & Ward, 2005; Zarnetske et al., 2007; Stofleth et al., 2008). It has also been suggested that hydraulic parameters or metrics correlate to Darcy's channel friction factor, f, and unit stream power, ω [N m^{-3}], which are simple measures of channel characteristics (Hart et al., 1999; Harvey & Wagner, 2000; Harvey et al., 2003; Stofleth et al., 2008; Zarnetske et al., 2007).

Darcy's channel friction and unit stream power is calculated by:

$$f = 8\mathrm{gds}/u^2 \tag{1.10}$$

where

g	gravitational acceleration
d	stream depth
s	streambed slope
u	stream velocity

$$\omega = \gamma \mathrm{sQ/w} \tag{1.11}$$

where

γ	specific weight of water
w	mean channel width

Relationships have been reported with the exchange coefficient, α, as having a positive correlation with discharge (D'Angelo et al., 1993; Harvey et al., 1996; Hart et al., 1999; Wondzell, 2006; Zarnetske et al., 2007), negative correlation with discharge (Hart et al., 1999), no correlation with discharge (Scordo & Moore, 2009), and then having a negative correlation with friction factor and a positive correlation with unit stream power (Zarnetske et al., 2007). The cross-section area of the storage zone, A_s, has been reported to have a negative correlation with discharge (D'Angelo et al., 1993; Harvey et al., 1996; Valett et al., 1996), with positive correlation with discharge (Hart et al., 1999; Jin & Ward, 2005), and no correlation (Scordo & Moore, 2009). Due to these conflicting results, Wondzell & Swanson (1996) suggested that these apparent changes or correlations with discharge may be the product of the experimental method.

To help constrain the variability of A_s researchers tried to use the relative storage area, A_s/A, for stream comparison and found, negative correlations with discharge (D'Angelo et al., 1993, Valett et al., 1996; Morrice et al., 1997), no correlations with discharge (Hart et al., 1999; Jin & Ward, 2005), positive correlations with discharge (Scordo & Moore, 2009), and also positive correlations with friction factor (Harvey & Wagner, 2000; Jin & Ward, 2005). However, some of the correlations were not strong and displayed notable variation.

The retention factor, R_h, has been reported as having a negative correlation (Harvey et al., 2003; Jin & Ward, 2005; Zarnetske et al., 2007), no correlation (Scordo & Moore, 2009), and a positive correlation with friction and a negative correlation with unit stream power (Zarnetske et al., 2007). The uptake length, Ls, has been reported as a positive correlation with discharge (Valett et al., 1996; Jin & Ward, 2005; Scordo & Moore, 2009). The fraction of the median travel time due to transient storage, F_{med}, was reported as a negative correlation with discharge (Jin & Ward, 2005).

2. STUDY AREA

The study area includes the Dry Creek Experimental Watershed (DCEW) and nine tributary watersheds to the North Fork Boise River (TNFB) (Figure 2.1) in Idaho. The DCEW is approximately located 9 km northeast of Boise, Idaho and is part of the semi-arid southwestern region of Idaho. The nine tributary streams of the North Fork Boise River are approximately located 25 km west of Idaho City in the Boise River Basin. The study area, DCEW and the TNFB, are part of the Atlanta Lobe of the Cretaceous aged Idaho Batholith, consisting of highly erodible granite rock and steep topography, which extends approximately 275 km long and 130 km wide (Johnson et al., 1988). The area has topography that is moderately sloped and strongly shaped by streams. The soils in the area range from loam to sandy loam with cobbles and boulders in texture and have high surface erosion potential (USDA, 1997). The characteristics of the ten streams and affiliated basins are presented in Table 2.1.

The climate is characterized by typically cold, wet winters and with freezing temperatures, and hot, dry summers. Precipitation ranges from about 600 to 1,000 mm per year, with the higher elevations receiving the greater amounts and the majority of the precipitation falling as snow in the winter with occasional spring storms.

Table 2.1. Stream/Basin characteristics obtained from StreamStats (USGS), June 14, 2010.

Stream	Drainage Area (km^2)	Min. Basin Elevation (m)	Max Basin Elevation (m)	Mean Basin Slope (%)	Forest Cover (%)	Mean Precip. (cm)
Little Beaver	40.9	1542.7	2054.9	23.3	48.6	79.8
Pikes Fork	25.1	1634.1	2332.3	33.0	60.8	82.8
Banner	22.8	1618.9	2073.2	26.1	54.4	77.2
Big Owl	18.1	1362.8	2012.2	33.9	36.9	73.7
Hungarian	11.4	1277.4	2167.7	44.2	32.3	63.5
German	23.1	1381.1	2393.3	48.6	40.9	67.6
Beaver	14.5	1298.8	2088.4	47.6	49.2	65.0
Trail	19.4	1475.6	2658.5	41.5	53.5	72.4
Hunter	16.3	1475.6	2707.3	44.0	48.7	70.9
Dry Creek	27.1	1027.4	2137.2	46.0	46.0	71.1

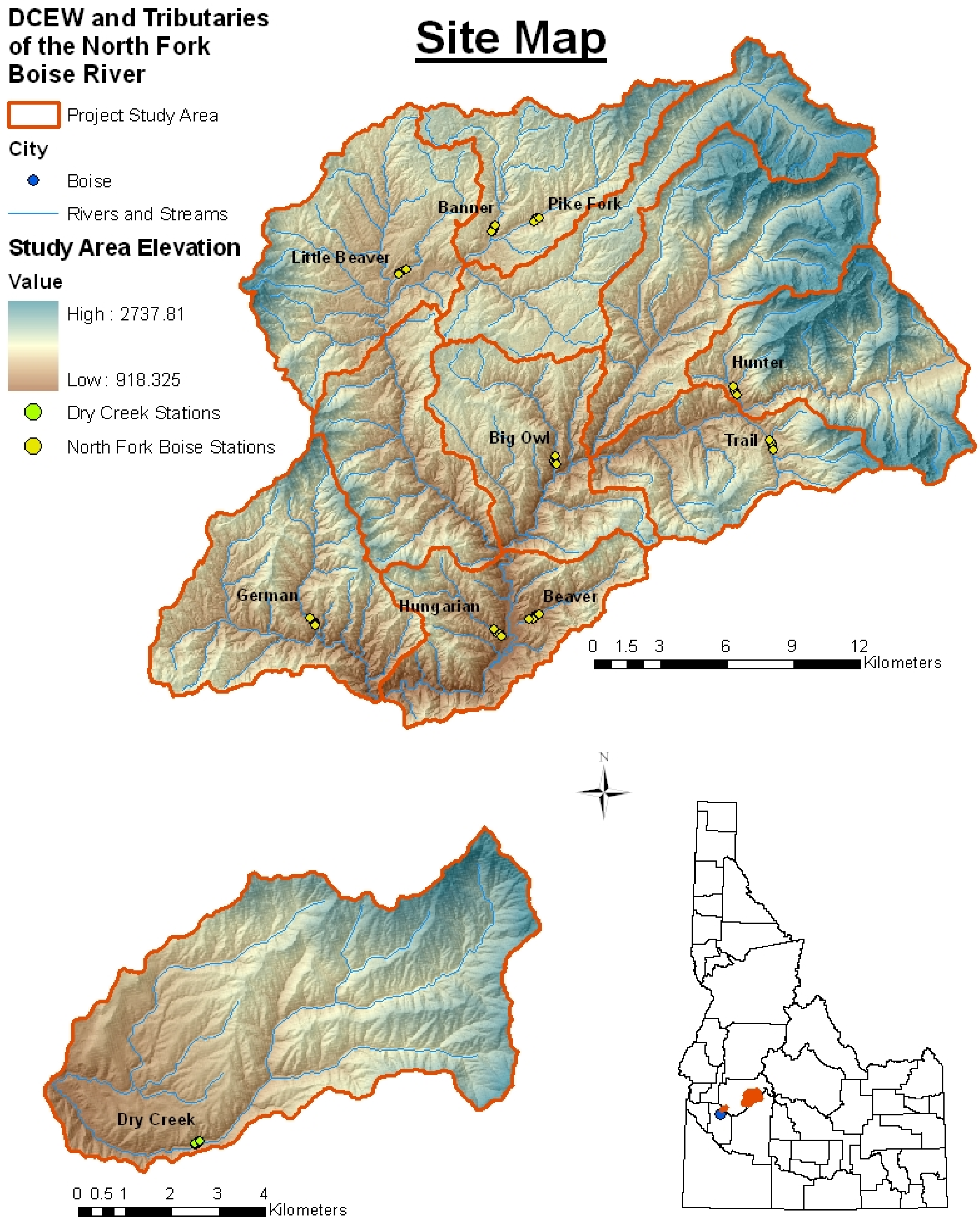

Figure 2.1. Site Map

3. METHODS

Stream tracer experiments were conducted in ten different streams over a period of time where a conservative solute, rhodamine WT, was measured in the stream channel, which resulted in breakthrough curves that show the concentration over time during the experiment. The breakthrough curves were then inversely modeled with OTIS, the common mathematical code used by the U.S Geological Survey for parameterizing hyporheic exchange to obtain optimal parameter sets that were analyzed for relationships to discharge, velocity, friction factor, and to stream unit power.

3.1 Tracer Experiments

Stream tracer experiments were conducted on approximately 100m sections of the streams throughout the study period. Each tracer consisted of continuous injection of Rhodamine WT (RWT) into a stream location that promoted complete mixing vertically and horizontally in the stream by the time the solute reached the study reach. The appropriate RWT mass of the injection was determined by mixing calculations with the goal plateau concentration to be around 50 ppb. At the end of each study reach, in situ stream RWT concentrations were measured continuously with either a Hach HydroLab DS5X connected to a Turner Designs fluorometer or an YSI 6820 V2 Sonde outfitted with the YSI 6130 rhodamine sensor. The injection and downstream sampling points were the same for all study reaches when there were repeated experiments. Rhodamine WT was used due to its conservative nature, although it is not completely conservative because of its nature to absorb to streambed material. The sorption and desorption of the RWT was not taken into account with the simulations and it was assumed that any sorption would be minor and similar from experiment to experiment.

Tracer experiments in DCEW started November 26, 2008 and spanned across dates to Aug 27, 2009, collecting data from seasonal changes. Tracer experiments in DCEW were designed to develop a temporal model of how transient storage parameters and metrics changed over time with seasonal changes. Experiments on the TNFB sites started September 1, 2008 and completed September 21, 2008 to have flows in each stream relative to the others. TNFB tracer experiments were done to understand what spatial variability exists in the transient storage parameters and their associated metrics when different streams with similar characteristics are compared to each other. Each tracer experiment was run until the concentration plateau, around 50 ppb, was reached with consecutive repeat experiments holding the plateau longer each time.

3.2 Piezometers and Vertical Head Gradients

Piezometers were installed in the DCEW study area to measure vertical head gradients throughout the study period. The piezometer pipes consisted of plastic 1/2 inch PVC pipe with a 5cm slot zone screened with nylon mesh that were installed to depths of 5, 10, and 15 cm into the streambed sediments that were in or near the thalweg of the stream. Thirteen piezometer nests were installed in Dry Creek. Occasionally, a piezometer would be washed out of the nest, creating gaps in data collection. New piezometers were installed if any were missing and data collection for the newly installed piezometer would occur during the next experiment to allow the piezometer to reach equilibrium. During the spring of 2008, the water flows were very high and washed out the majority of the nest. Nests were reinstalled as close to the previous spots, but only included the 5 and 15 cm piezometers.

Water levels in the piezometer were measured using a stick that was outfitted with electrical contacts at the end of the stick connected to a buzzer that sounded when contact was made with the water surface. A tape measure was also attached to the stick to get the measurement of the surface water when the buzzer sounded. Vertical head gradients (VHG) were calculated using:

$$\mathrm{VHG} = \frac{\Delta \mathrm{h}}{\Delta \mathrm{l}} \tag{3.1}$$

where Δh is the elevation difference between the water surface inside the piezometer and the water surface of the stream and Δl is the distance between the surface of the stream bed and the slot zone (Baxter et al., 2003). Up-welling hyporheic flow will cause a positive vertical head gradient whereas down-welling flow causes a negative vertical head gradient. Neutral piezometers were defined by Guenther (2007) as having $|\mathrm{VHG}|$ <0.05cm cm^{-1}, which covers the bounds of uncertainty in the measurements. Gradients that were of <.05 cm/cm> were assumed to be within the range of error for this study as well.

3.3 Simulation Solute Transport with the Transient Storage Model

The One-dimensional Transport with Inflow and Storage with Parameters estimation (OTIS-P) model was used to simulate the breakthrough curves of all experiments (Runkel, 1998). OTIS-P solves the transient storage model by inverse modeling of the tracer data using a non-linear least-squares optimization routine that runs the code numerous times to find the best-fit parameters for the cross-sectional area of the channel, A, dispersion coefficient, D, stream storage exchange coefficient, α, cross-sectional area of the storage zone, A_s, that reproduce the breakthrough curves. The modeling of the parameters was accomplished first by using OTIS and estimates of the hydraulic parameters to achieve a good visual fit of the breakthrough curves, which were then plugged into OTIS-P to optimize the values and achieve convergence. A model run was accepted as a good fit when the four parameters would reproduce the breakthrough curves with a parameter and residual sum of squares convergence occurring twice consecutively and having less than .01% change from the previous run in parameter values.

Each run was checked for the sensitivity of the breakthrough curves to the transient storage model process by calculating the Damkohler number (DaI). The range of DaI for all the data was 1.23 to 10.63, which falls into the acceptable range of values for transient storage model processes.

3.4 Metrics Characterizing Transient Storage

Metrics related to hyporheic processes were used along with the transient storage model parameters to find correlations. The metrics used for comparisons are the relative storage size, A_s/A, storage exchange flux, q_s, average resident time in storage, t_s, uptake length, L_s, retention factor, R_h, and then the fraction of median travel time due to storage at 200m, F_{med}^{200}. The definitions and calculations of the metrics can be found in the background section. These metrics along with the hydraulic parameters were compared with the flow, Q, velocity, u, Darcy's friction factor, *f*, and unit stream power, ω, which are simple stream channel descriptions.

3.5 Relationships between Otis Parameters and Stream Properties

Pearson product-moment correlation was used to compare the relationship between the hydraulic parameters, and metrics with flow, velocity, Darcy's friction factor, and unit stream power. The square of the correlation coefficients, r^2 values, were considered to have a strong correlation when values were >.75, considerable correlation with values .75-.50, slight correlation with values .50-.25, and minor correlation <.25. T-tests were performed with the correlation coefficient to calculate the significance of the correlation with the following equation:

$$t = \frac{r\sqrt{n-2}}{\sqrt{1-r^2}} \quad (3.2)$$

where r is the correlation coefficient and n is the number of samples (Davis, 1986). This t value then can be put into the students t distribution to find the p value (significance) according to the degree of freedom, n-2. A correlation was considered significant when $p < 0.05$.

4. RESULTS

Figure 4.1 shows an example of a breakthrough curve that was modeled through OTIS-P. The breakthrough curves were collected over a range of discharges in the Dry Creek Experimental Watershed (DCEW) that ranged from 0.0073 to 0.5007m^3/s (Appendix C, Table C.1). Mean velocity during the tracer experiments in the DCEW ranged from 0.0741 to 0.7474m/s. Discharges during the tracer experiments in the

Tributary streams of North Fork Boise River (TNFB) ranged from 0.0138 to 0.1021m^3/s (Appendix C, Table C.3). Mean velocity during the tracer experiments in the TNFB ranged from 0.0490 to 0.2591m/s. Discharge and velocity were the lowest during the early fall, which coincides with the lowest rainfall and highest temperatures.

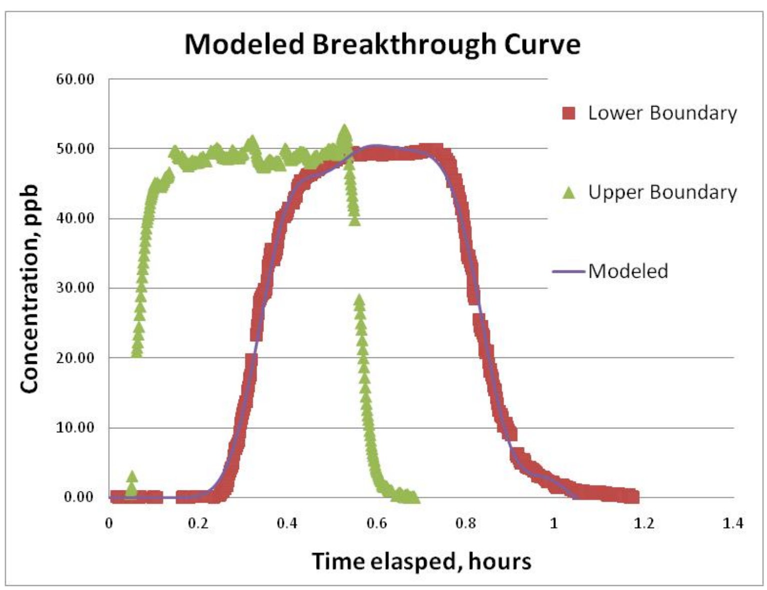

Figure 4.1. Example of a Modeled Breakthrough Curve

4.1 Hydraulic Parameters and Metrics

Longitudinal dispersion in DCEW ranged from 0.0102 to 0.3888m^2/s. The cross-section of the channel in DCEW ranged from 0.0965 to 0.6879m^2 and the cross-section area of the storage zone in DCEW ranged from 0.0132 to 0.1608m^2. The exchange coefficient in DCEW ranged from 0.0004 to 0.0073s^{-1}. The channel area was consistently larger than the storage area. The hydraulic parameters, D, A, A_s, and α, were lower during the fall and higher during spring following the trend of the stream discharge (Figure 4.2).

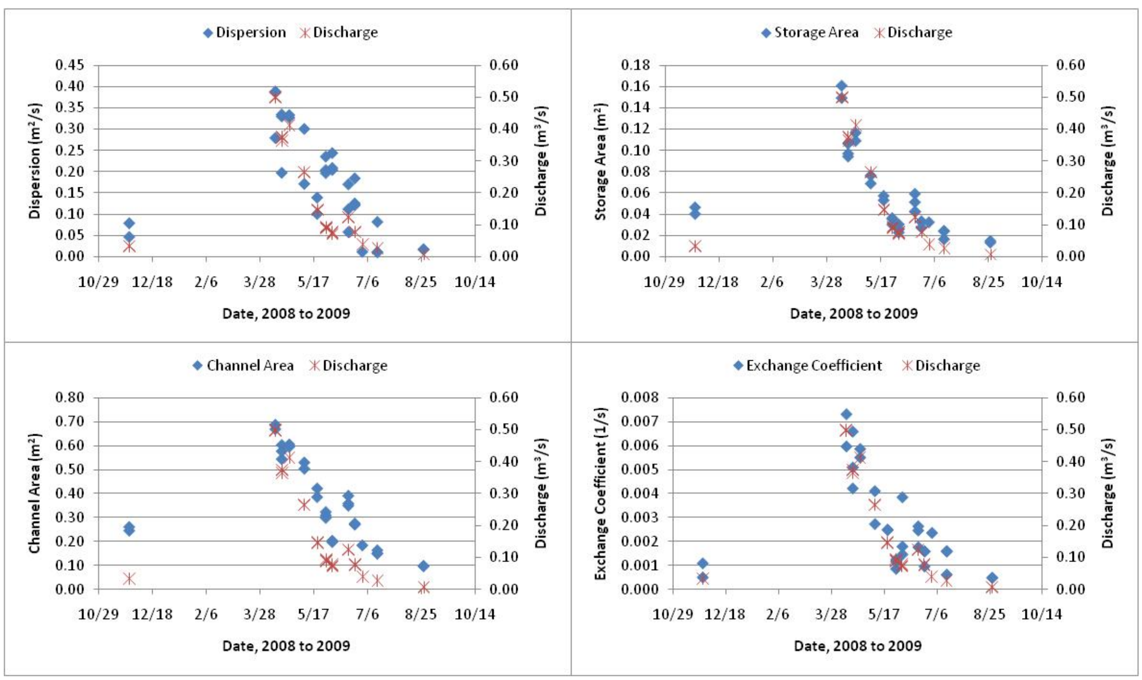

Figure 4.2. Temporal patterns of hydraulic parameters and discharge.

Storage exchange flux, q_s, in DCEW ranged from 0.0000459 to 0.0049m^3/s-m (Appendix C, Table C.2). Average resident time in storage, t_s, ranged from 29.7 to 318.5s in DCEW. Uptake length, L_s, ranged from 91.5 to 347.1m in the DCEW. The hydraulic retention, R_h, ranged from .2527 to 2.0218s/m in the DCEW. The fraction of median travel time due to transient storage at 200m, F_{med}^{200}, ranged from 4.42 to 16.62% in the DCEW. The relative storage area, A_s/A, ranged from .0992 to .2401m^2m^{-2} in the DCEW.

Longitudinal dispersion in the TNFB ranged from 0.0274 to 0.2830m^2/s. The cross-section of the channel in the TNFB ranged from 0.1291 to 0.4739m^2 and the cross-section area of the storage zone in the TNFB ranged from 0.0197 to 0.1162m^2. The exchange coefficient in the TNFB ranged from 0.0002 to 0.0018s^{-1}. The channel area was consistently larger than the storage area.

Storage exchange flux, q_s, in the TNFB ranged from 0.0000278 to 0.000563 (Appendix C, Table C.4). The average resident time in storage, t_s, ranged from 117.2 to 709.3s, the uptake length, L_s, ranged from 106.7 to 755.0m in the TNFB. The hydraulic retention, R_h, ranged from .6163 to 5.0154s/m, the fraction of median travel time due to transient storage at 200m, F_{med}^{200}, ranged from 2.80 to 18.44%, and the relative storage area, A_s/A, ranged from .1237 to .2785 m^2m^{-2} in the TNFB.

4.2 Vertical Head Gradients

The resulting head measurements from the piezometers were fairly small and were calculated to vertical head gradients. Figure 4.3 shows the vertical head gradients across the length of the reach as well as at the different times the measurements were taken. The majority of the measured points fall within the neutral boundary of $-.05<x>.05$, which consists of the measurement uncertainty. The data is temporally variable as most piezometer nests did not show a consistent vertical gradient favoring a down-welling or an up-welling area. Only in two locations are there a consistent down-welling through the seasonal changes. At piezometer nest 2, 21m downstream, the 15 cm deep piezometer showed a very good trend of down-welling as well as a steady gradient and the 5cm deep piezometer loosely showed this trend as well. At nest 9, 102 m downstream, the 15 cm deep piezometer had a fairly good trend for down-welling, whereas the 5cm piezometer was variable and trended to an up-welling area. No consistent up-welling areas were visible through the seasonal changes.

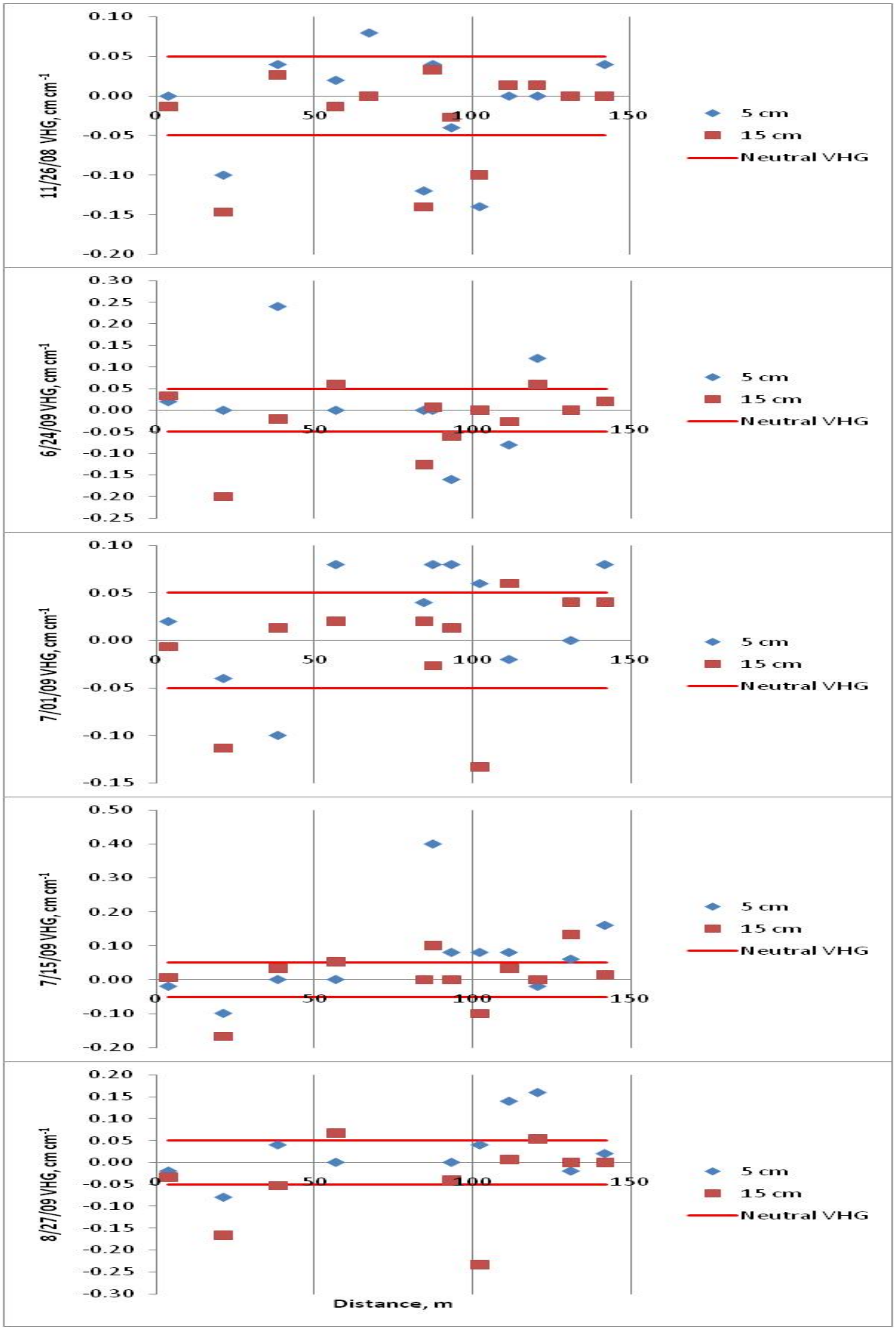

Figure 4.3. Vertical head gradients for the piezometers nests.

4.3 Correlations

Dispersion, D, is positively correlated for discharge, velocity, and unit stream power, and negatively correlated with friction factor (Appendix A, Fig A.1). When dispersion is compared to discharge, it ranged from slightly correlated (TNFB, R^2=.274, p-value=.037) to considerable correlation (DCEW, R^2=.654, p-value<.001) and significant with the full dataset being slightly correlated (R^2=.484, p-value<.001). Compared to velocity, it ranges from slightly correlated (TNFB, R^2=.2629, p-value=.042) to considerable correlation (DCEW, R^2=.75, p-value<.001) and significant with the full dataset being considerably correlated (R^2=.517, p-value<.001). Friction factor was only slightly correlated but significant for all data sets (TNFB, R^2=.266, p-value=.041) (DCEW, R^2=.347, p-value<.001) (Full dataset, R^2=.28, p-value<.001). Unit stream power ranged from minor correlation (TNFB, R^2=.07, p-value=.321) to considerable correlation (DCEW, R^2=.669, p-value<.001) and significant with the full dataset being slightly correlated (R^2=.487, p-value<.001).

Channel cross-section area, A, is positively correlated for discharge, velocity, and unit stream power, and negatively correlated with friction factor (Appendix A, Fig A.2). When compared to discharge, it ranged from considerable correlated (TNFB, R^2=.545, p-value=.001) to strongly correlated (DCEW, R^2=.922, p-value<.001) and significant with the full dataset being strongly correlated (R^2=.797, p-value<.001). Compared to velocity, it ranged from a minor correlation (TNFB, R^2=.016, p-value=.636) to a strong correlation (DCEW, R^2=.866, p-value<.001) with the full dataset being considerably correlated (R^2=.656, p-value<.001). Friction factor ranged from a minor correlation (TNFB, R^2=.001, p-value=.887) to slightly correlated (DCEW, R^2=.347, p-value=.001) with the full dataset being a minor correlation (R^2=.187, p-value=.002). Unit stream power ranged from a minor correlation (TNFB, R^2=.126, p-value=.178) to strongly correlated (DCEW, R^2=.939, p-value<.001) with the full dataset being strongly correlated (R^2=.784, p-value<.001).

Storage cross-section area, A_s, is positively correlated for discharge, velocity, and unit stream power, and negatively correlated with friction factor with the TNFB having no correlation with velocity, friction factor, and unit stream power (Appendix A, Fig A.3). When compared to discharge, it ranged from slightly correlated (TNFB, R^2=.281, p-value=.035) to strongly correlated (DCEW, R^2=.945, p-value<.001) with the full dataset being considerably correlated (R^2=.664, p-value<.001). Compared to velocity, it ranges from a minor correlation (TNFB, R^2=.001, p-value=.914) to a strong correlation (DCEW, R^2=.827, p-value<.001) with the full dataset being slightly correlated (R^2=.462, p-value<.001). There was only a minor correlation for friction factor in all the data sets (TNFB, R^2=.005, p-value=.796) (DCEW, R^2=.183, p-value=.016) (Full dataset, R^2=.069, p-value=.074). Unit stream power ranged from a minor correlation (TNFB, R^2=.004, p-value=.809) to strongly correlated (DCEW, R^2=.937, p-value<.001) with the full dataset being considerably correlated (R^2=.621, p-value<.001).

Exchange coefficient, α, is positively correlated for discharge, velocity, and unit stream power, and negatively correlated with friction factor with the TNFB having no correlation with unit stream power (Appendix A, Fig A.4). When compared to discharge, it ranged from slightly correlated (TNFB, R^2=.253, p-value=.047) to strongly correlated (DCEW, R^2=.866, p-value<.001) with the full dataset being strongly correlated (R^2=.868, p-value<.001). Compared to velocity, it ranged from a slight correlation (TNFB,

R^2=.252, p-value=.047) to a strong correlation (DCEW, R^2=.875, p-value<.001) with the full dataset being strongly correlated (R^2=.88, p-value<.001). Friction factor was only slightly correlated but significant for all data sets (TNFB, R^2=.281, p-value=.035) (DCEW, R^2=.273, p-value=.003) (Full dataset, R^2=.337, p-value<.001). Unit stream power ranged from a minor correlation (TNFB, R^2=.014, p-value=.664) to strongly correlated (DCEW, R^2=.863, p-value<.001) with the full dataset being strongly correlated (R^2=.793, p-value<.001).

Storage exchange flux, q_s, is positively correlated for discharge, velocity, and unit stream power, and negatively correlated with friction factor with the TNFB having no correlation with unit stream power (Appendix A, Fig A.5). When compared to discharge, it ranged from considerably correlated (TNFB, R^2=.553, p-value=.001) to strongly correlated (DCEW, R^2=.959, p-value<.001) with the full dataset being strongly correlated (R^2=.959, p-value<.001). Compared to velocity, it ranged from a minor correlation (TNFB, R^2=.205, p-value=.047) to a strong correlation (DCEW, R^2=.875, p-value<.001) with the full dataset being strongly correlated (R^2=.86, p-value<.001). Friction factor was only a minor correlation for all data sets (TNFB, R^2=.179, p-value=.102) (DCEW, R^2=.188, p-value=.015) (Full dataset, R^2=.226, p-value=.001). Unit stream power ranged from a minor correlation (TNFB, R^2=.058, p-value=.367) to strongly correlated (DCEW, R^2=.947, p-value<.001) with the full dataset being strongly correlated (R^2=.887, p-value<.001).

Average time in storage, t_s, is negatively correlated for discharge, velocity, and unit stream power, and positively correlated with friction factor (Appendix A, Fig A.6). When compared to discharge, it was only slightly correlated but significant for all data sets (TNFB, R^2=.291, p-value=.031) (DCEW, R^2=.348, p-value<.001) (Full dataset, R^2=.263, p-value<.001). Compared to velocity, it ranged from a minor correlation (TNFB, R^2=.247, p-value=.05) to a considerable correlation (DCEW, R^2=.543, p-value<.001) with the full dataset being slightly correlated (R^2=.40, p-value<.001). Friction factor ranged from minor correlated (TNFB, R^2=.178, p-value=.103) to strongly correlated (DCEW, R^2=.886, p-value<.001) with the full dataset being a considerable correlation (R^2=.532, p-value<.001). Unit stream power ranged from a minor correlation (TNFB, R^2=.102, p-value=.228) to slightly correlated (DCEW, R^2=.379, p-value<.001) with the full dataset being minor correlated (R^2=.244, p-value<.001).

Uptake length, L_s, is negatively correlated for discharge, velocity, and unit stream power, and positively correlated with friction factor with the TNFB having no correlation with discharge, velocity, friction factor, or unit stream power (Appendix A, Fig A.7). When compared to discharge, velocity, friction factor, and unit stream power, the correlations were all minor correlations for all data sets (Appendix A & B).

Retention Factor, R_h, is negatively correlated for discharge, velocity, and unit stream power, and positively correlated with friction factor (Appendix A, Fig A.8). When compared to discharge, it ranged from a minor correlation (TNFB, R^2=.199, p-value=.083) to a considerable correlation (DCEW, R^2=.288, p-value=.002) with the full dataset showing a minor correlation (R^2=.196, p-value=.002). Compared to velocity, it ranged from a slight correlation (DCEW, R^2=.486, p-value<.001) to a considerable correlation (TNFB, R^2=.55, p-value=.001) with the full dataset being slightly correlated (R^2=.359, p-value<.001). Friction factor ranged from slightly correlated (TNFB, R^2=.298, p-value=.029) to strongly correlated (DCEW, R^2=.929, p-value<.001) with the full dataset being considerably correlated (R^2=.566, p-value<.001). With unit stream power, there was only a slight, but significant correlation (TNFB, R^2=.288, p-value=.032) (DCEW, R^2=.323, p-value=.001) (Full dataset, R^2=.243, p-value<.001).

Fraction of median travel time due to storage at 200m, F_{med}^{200}, was only significantly correlated to DCEW dataset (Appendix A, Fig A.9). When compared to discharge, velocity, and unit stream power, DCEW had a slight correlation and no correlation with friction factor (Appendix A & B). The TNFB had minor to no correlation with discharge, velocity, friction factor, and unit stream power.

Relative storage size, A_s/A, was positively correlated for the DCEW data set to discharge, velocity, and unit stream power, and minor to no correlations for the TNFB and full dataset to discharge, velocity, friction factor, and unit stream power (Appendix A, Fig A.10). When compared to discharge, it ranged from no correlation (TNFB, R^2=.001, p-value=.929) to a slight correlation (DCEW, R^2=.437, p-value<.001) with the full dataset having no correlation (R^2=.040, p-value=.18). Compared to velocity, it ranged from no correlation (TNFB, R^2=.015, p-value=.655) to a slight correlation (DCEW, R^2=.311, p-value=.001) with the full dataset having no correlation (R^2=.002, p-value=.745). Friction factor had no correlations (TNFB, R^2=.025, p-value=.556) (DCEW, R^2=.003, p-value=.779) (Full dataset, R^2=.029, p-value=.253). Unit stream power ranged from having a minor correlation (TNFB, R^2=.102, p-value=.228) to a slight correlation (DCEW, R^2=.409, p-value<.001) with the full dataset having no correlation (R^2=.027, p-value=.268).

5. DISCUSSION

Variability exists within the temporal data (DCEW) and within the spatial data (TNFB). Figures 1 through 4 in Appendix A shows that the DCEW data has a positive linear trend with discharge, but the degree of correlation varies on the different parameters. Looking more closely at the figures shows that parameters that are similar in discharge can vary in value, such is the case with dispersion and the exchange coefficient, where there is a degree of variation that discharge cannot fully explain. The spatial data varies more than the temporal data because it does not correlate as well with discharge. This variation could be due to processes that are occurring in the stream that are site specific, such as the amount of debris or litter in the main channel that could be increasing the storage parameters without actually increasing the hyporheic exchange but increasing the surface water storage. Using only the one lumped storage parameters make it hard to differentiate the causes for the variability. So it can be assumed that using the one lumped storage parameters will have a greater amount of variability because it is lumping several processes, main channel and hyporheic, into one data value.

The exchange coefficient, α, looks as if it is mainly influenced by discharge with very little regard to spatial change, whereas the storage cross-sectional area seems to be more site specific with a much higher amount of variability. This may be the case where some main channel processes aren't contributing much to the value of alpha, but without more data collected at higher flows at the TNFB, sites it can only be conjectured that the exchange coefficient could be contributed mainly to discharge. Data would need to be collected at higher flows to see if the correlation follows as closes as the DCEW data does.

This variability can be discussed with another data set that was collected with the same methods, but was collected at Cottonwood Creek in Boise, Idaho. This test reach was unique to the other ones because the reach was a concrete canal with similar flows. Stream tracer experiments were ran to see if storage cross-section area, A_s, and the exchange coefficient, α, would be needed to model the curves. Modeled runs without the transient storage parameters resulted in non-convergence and thus no modeled results. Modeled runs with the transient storage parameters resulted in convergence and values. Table C.5 and C.6 in Appendix C, show the resulting values for the Cottonwood Creek experiment. Figure 5.1 shows where the Cottonwood values fall within the DCEW and the TNFB data sets when compared to discharge. In the concrete canal of Cottonwood Creek, the storage cross-section area, A_s, is lower than the rest of the data values, which it should be since it has no hyporheic area due to the concrete lining. The small amount of storage it does have could be the result of minor amounts of sand and plant life at the very bottom of the canal. The exchange coefficient, α, is higher than the DCEW and TNFB data values, which makes sense for the concrete canal since higher values of alpha means that the solute is spending less time in storage, which is what one would expect as very little if any storage in a concrete canal would exist. The Cottonwood data really shows that the lumped storage parameters will cause variability and error due to in-channel processes.

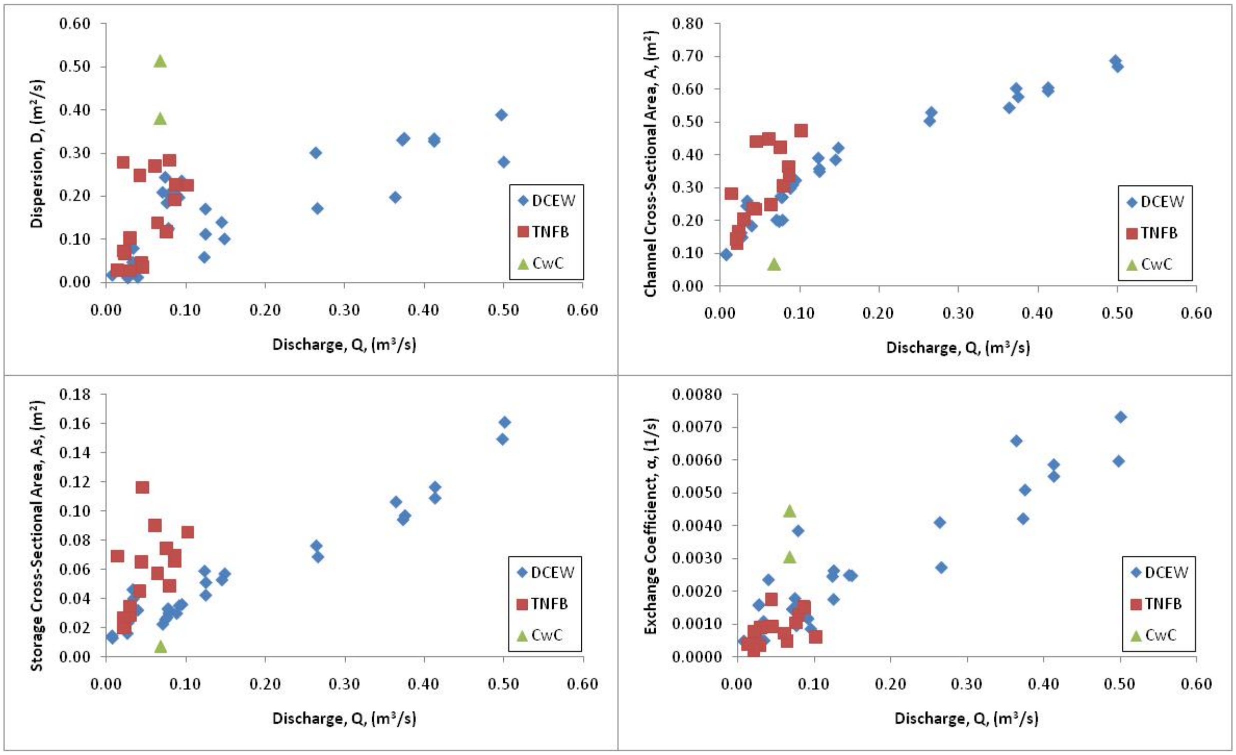

Figure 5.1. Cottonwood Creek data added to DCEW and TNFB data.

To use the parameters to characterize a stream reach one would expect the values of the parameters to have low temporal variability and have high spatial variability in order to be a good description of streams. This is not the case with the hydraulic parameters where there was a high amount of temporal variability as well as spatial variability. As previously mentioned though, the exchange coefficient, α, still might be able to characterize a stream. However, the site characterization with α would be a range of values that would be expected at different flows and would describe the hyporheic exchange for a certain type of stream. In this research, streams were chosen with similar alluvium, slope, discharge, and order. Preliminary results may suggest that α may be used as a reach characterization with using a stream classification that would group streams together that share similarities. This of course is conjecture and needs further study.

A high amount of variability was found in the vertical head gradients of the piezometer nests, which could be the product of reality or sensitivity of river processes and measurement error. As discussed previously, only two nests have any consistent gradient through the seasonal changes. Piezometer nests are usually used to physically show that hyporheic exchange occurs within the sediments. Results from this study are inconclusive for the vertical head gradients due to the instability of the piezometers in the sediments.

Researchers have compared their data to the Harvey and Wagner (2000) plot of A_s/A versus friction factor to validate their data if it falls within their correlation. The DCEW and TNFB data have a range of .099 to .279 for the relative storage size, A_s/A, and .83 to 30.65 for friction factor, *f*, which falls nicely into the correlated plot by Harvey and Wagner, which shows the data with a positive trend that the US reaches have with the relative storage size verse friction factor.

Researchers have presented conflicting findings of how the hydraulic parameters correlate to discharge and to other channel descriptors. I have added my findings as well to this list. Although, I do suggest that the conflicting findings are due to the variability of the parameters caused from the lumping of the processes of the stream. Plots that correlate the data need to correlate that data over large enough scales in order to overcome the variability that is caused by lumping the stream processes into one parameter. An example of this suggestion can be found with the plot of A_s/A vs. friction factor. The correlation of the A_s/A to the friction factor from this study is poor, but when this data is added to the much larger Harvey and Wagner (2000) plot that incorporates several studies over a very broad spectrum of friction factors, the TNFB and DCEW data falls into the correlation that Harvey and Wagner had found. This may be the reason for having conflicting correlations presented by researchers; not enough data was collected over a large enough scale for a correlation to be made with the data variation in mind. Mainly, the data may vary on the scale on which it was correlated.

6. CONCLUSION

Temporal variation of the OTIS parameters at a stream reach is primarily governed by changes in discharge. When comparing spatially different but similar sites, the correlation of discharge to the hydraulic parameters weakens to a slight correlation, showing that a temporal regression model does not account for the variability of the parameters at different reaches. The spatial correlations showed that even though discharge was a contributing factor to stream and hyporheic processes, there were other site specific contributing factors that the one lumped storage transient storage model does not account for. The one lumped storage transient storage model creates variability in the data by lumping the channel and hyporheic processes resulting in parameters that are more site specific.

The use of the simple channel descriptors, such as the friction factor or unit stream power, does not improve the correlations significantly for temporal or spatial changes. It shows that simple channel descriptions are not capturing the majority of the hydraulic influences that occur for the stream and the hyporheic processes.

The stream tracer experiments and modeling results from the concrete canal of Cottonwood Creek showed that the storage parameters A_s and α still had to be used in order to model a stream reach primarily dominated by advection and dispersion processes. Having the need to use the storage parameters to model the data might suggest that there is a small portion of the parameters that are mathematical artifacts of the modeling process. Caution needs to be used with hydraulic parameters that are from restrictive environments where hyporheic processes would be believed to be little or null.

Preliminary results showed that α may not spatially change across streams that are similar in characterization. Further research needs to be done to see if spatially different, but similar streams result in the same temporal trend of the exchange coefficient, α. If this were done, α may be used as a stream reach characterization when coupled with a stream classification that groups streams together with similar alluvium, slope, discharge, and order.

REFERENCES

Anderson, J.K., Wondzell, S.M., Gooseff, M.N., and Haggerty, R. (2005). Patterns in stream longitudinal profiles and implications for hyporheic exchange at the H.J. Andrews Experimental Forest, Oregon, USA. Hydrological Processes. 19, 2931-2949.

Baxter, C.V., and Hauer F.R. (2000). Geomorphology, hyporheic exchange, and selection of spawning habitat by Bull Trout. Canada Journal of Fishery Aquatic Science. 57, 1470-1481.

Baxter, C.V., F.R. Hauer, and W.W. Woessner, (2003). Measuring groundwater-stream water exchange: new techniques for installing mini-piezometers and estimating hydraulic conductivity. Transactions of the American Fisheries Society. 132, 493-502.

Bencala, K.E., and Walters, R.A. (1983). Simulation of solute transport in a mountain pool-and-riffle stream: A transient storage model. Water Resources Research. 19 (3), 718-724.

Boulton, A.J., Findlay, S., Marmonier, P., Stanely, E.H., and Valett, H.M. (1998). The functional significance of the hyporheic zone in streams and rivers. Annual Reviews of Ecology Systems. 29, 59-81.

Briggs, M.A., Gooseff, M.N., Arp, C.D., and Baker, M.A. (2009). A method for estimating surface transient storage parameters for streams with concurrent hyporheic storage. Water Resources Research. 45, 1-13.

Buffington, J.M., and Tonina, D. (2009). Hyporheic exchange in mountain rivers II: Effects of channel morphology on mechanics, scales, and rate of exchange. Geography Compass. 3, 1-25.

Choi, J., Harvey, J.W., and Conklin, M.H. (2000). Characterizing multiple timescales of stream and storage zone interaction that affect solute fate and transport in streams. Water Resources Research. 36(6), 1511-1518.

D'Angelo, D.J., Webster, J.R., Gregory, S.V., and Meyer, J.L. (1993). Transient storage in Appalachian and Cascade Mountain streams as related to hydraulic characteristics. Journal of the North American Benthological Society. 12(3), 223-235.

Davis, J.C. (1986). Statistic and data analysis in geology. John Wiley & Son, Inc. New York, New York.

Ensign, S.H., and Doyle, M.W. (2005). In-channel transient storage and associated nutrient retention: Evidence from experimental manipulations. Limnology and Oceanography. 50(6), 1740-1751.

Findlay, S. (1995). Importance of surface-subsurface exchange in stream ecosystems: The hyporheic zone. Limnology and Oceanography. 40(1), 159-164.

Findlay, S., Strayer, D., Goumbala, C., and Gould, K. (1993). Metabolism of streamwater dissolved organic carbon in the shallow hyporheic zone. Limnology and Oceanography. 38(7), 1493-1499.

Guenther, S. (2007). Headwater stream temperature response to alternative riparian management: An Experimental heat budget approach. Master Thesis, University of British Columbia, Vancouver, BC.

Hart, D.R., Mulholland, P.J., Marzolf, D.L., DeAngelis, D.L.., and Hendricks, S.P. (1999). Relationships between hydraulic parameters in a small stream under varying flow and seasonal conditions. Hydrological Processes. 13, 1497-1510.

Harvey, J.W., and Bencala, K.E. (1993). The effect of streambed topography on surface-subsurface water exchange in mountain catchments. Water Resources Research. 29 (1), 89-98.

Harvey, J.W., Conklin, M.H., and Koelsch, R.S. (2003). Predicting changes in hydrologic retention in an evolving semi-arid alluvial stream. Advances in Water Resources. 26, 939-950.

Harvey, J.W., Wagner, B.J., and Bencala, K.E. (1996). Evaluating the reliability of the stream tracer approach to characterize stream-subsurface water exchange. Water Resources Research. 32 (8), 2441-2451.

Harvey, J.W., and Wagner, B.J. (2000). Quantifying hydrologic interactions between streams and their subsurface hyporheic zones. In: Streams and Ground Waters (Jones, J.A., and Mulholland, P.J., eds). Academic Press, San Diego, 1-44.

Hynes, H.B.N. (1974). Further studies on the distribution of stream animals within the sub-stratum. Limnology and Oceanography. 19, 92-99.

Hynes, H.B.N. (1975). The stream and its valley. Verhandlungen der Internationalen Vereinigung fur theoretische und angewandte. Limnologie. 19:1–15.

Jin, H.S., and Ward, G.M. (2005). Hydraulic characteristics of a small coastal plain stream of the southeastern united states: effects of hydrology and season. Hydrological Processes. 19, 4147-4160.

Johnson, K.M., Lewis R.S., Bennett, E.H., and Kiilsgaard, T.H. (1988). Cretaceous and Tertiary intrusive rocks of south-central Idaho. In: Guidebook to the Geology of Central and Southern Idaho (Link, P.K. and Hackett, W.R., eds.). Idaho Geological Survey, Bulletin 27, 55-86.

Mallard, F., Tockner, K., Dole-Oliver, M.J., and Ward, J.V. (2002). A landscape perspective of surface-subsurface hydrological exchange in river corridors. Freshwater Biology. 47, 621-640

Morrice, J.A., Valett, H.M., Dahm, C.N., and Campana, M.E. (1997). Alluvial characteristics, groundwater-surface water exchange and hydrological retention in headwater streams. Hydrological Processes. 11, 253-267.

Lautz, L.K., Siegel, D.I., and Bauer, R.L. (2006). Impact of debris dams on hyporheic interaction along a semi-arid stream. Hydrological Processes. 20, 183-196.

Runkel, R.L. (1998). One-dimensional transport with inflow and storage (OTIS): A solute transport model for streams and rivers. Water-Resources Investigations (US Geological Survey) Report, 98-4018.

Runkel, R.L. (2002). A new metric for determining the importance of transient storage. Journal of the North American Benthological Society. 21(4), 529-543.

Scordo, E.B., and Moore, R.D. (2009). Transient storage processes in a steep headwater stream. Hydrological Processes. 23, 2671-2685.

Stofleth, J.M., Shields, F.D., and Fox, G.A. (2008). Hyporheic and total transient storage in small, sand-bed streams. Hydrological Processes. 22, 1885-1894.

Storey, R.G., Howard, K.W.F., and Williams, D.D. (2003). Factors controlling riffle-scale hyporheic flows and their seasonal changes in a gaining stream: A three-dimensional groundwater flow model. Water Resources Research. 39 (2), 1034-1061.

Stream Solute Workshop. (1990). Concepts and methods for assessing solute dynamics in stream ecosystems. Journal of the North American Benthological Society. 9(2), 95-119.

StreamStats (USGS). [Online Computer Software]. http://streamstats.usgs.gov/gages/. Retrieved (June, 14, 2010).

Tonina, D., and Buffington, J.M. (2007). Hyporheic exchange in gravel bed rivers with pool-riffle morphology: Laboratory experiments and three-dimensional modeling. Water Resources Research. 43, 1421-1437.

Triska, F.J., Kennedy, V.C., Avanzino, R.J., Zellweger, G.W., and Bencala, K.E. (1989). Retention and transport of nutrients in a third-order stream in northwestern California: Hyporheic processes. Ecology. 70 (6), 1893-1905.

USDA. (1997). Soil Survey of the Boise Front: Interim and supplemental report, Natural Resource Conservation Service, Boise, Idaho.

Valett, H.M., Fisher, S.G., and Stanley, E.H. (1990). Physical and chemical characteristics of the hyporheic zone of a sonorant desert stream. Journal of the North American Benthological Society. 9 (3), 201-215.

Valett, H.M., Morrice, J.A., Dahm, C.N., and Campana, M.E. (1996). Parent lithology, surface-groundwater exchange, and nitrate retention in headwater streams. Limnology and Oceanography. 41(2), 333-345.

Wagner, B.J., and Harvey, J.W. (1997). Experimental design for estimating parameters of rate-limited mass transfer: Analysis of stream tracer studies. Water Resources Research. 33(7), 1731-1741.

White, D.S. (1993). Perspectives on defining and delineating Hyporheic zones. Journal of the North American Benthological Society. 12 (1), 61-69.

White, D.S., Elzing, D.H., and Hendricks, S.P. (1987). Temperature patterns within the hyporheic zone of a northern Michigan River. Journal of the North American Benthological Society. 6 (2), 85-91.

Wondzell, S.M. (2006). Effect of morphology and discharge on hyporheic exchange flows in two small streams in the Cascade Mountains of Oregon, USA. Hydrologcial Processes. 20, 267-287.

Wondzell, S.M., and Swanson, F.J. (1996). Seasonal and storm dynamics of the hyporheic zone of a 4^{th}-order mountain stream. I: Hydrologic processes. Journal of the North American Benthological Society. 15, 3-19.

Zarnetske, J.P., Gooseff, M.N., Brosten, T.R., Bradford, J.H., McNamara, J.P., and Bowden, W.B. (2007). Transient storage as a function of geomorphology, discharge, and permafrost active layer conditions in Arctic tundra streams. Water Resources Research. 43, 1-13.

APPENDIX A

Correlation Charts

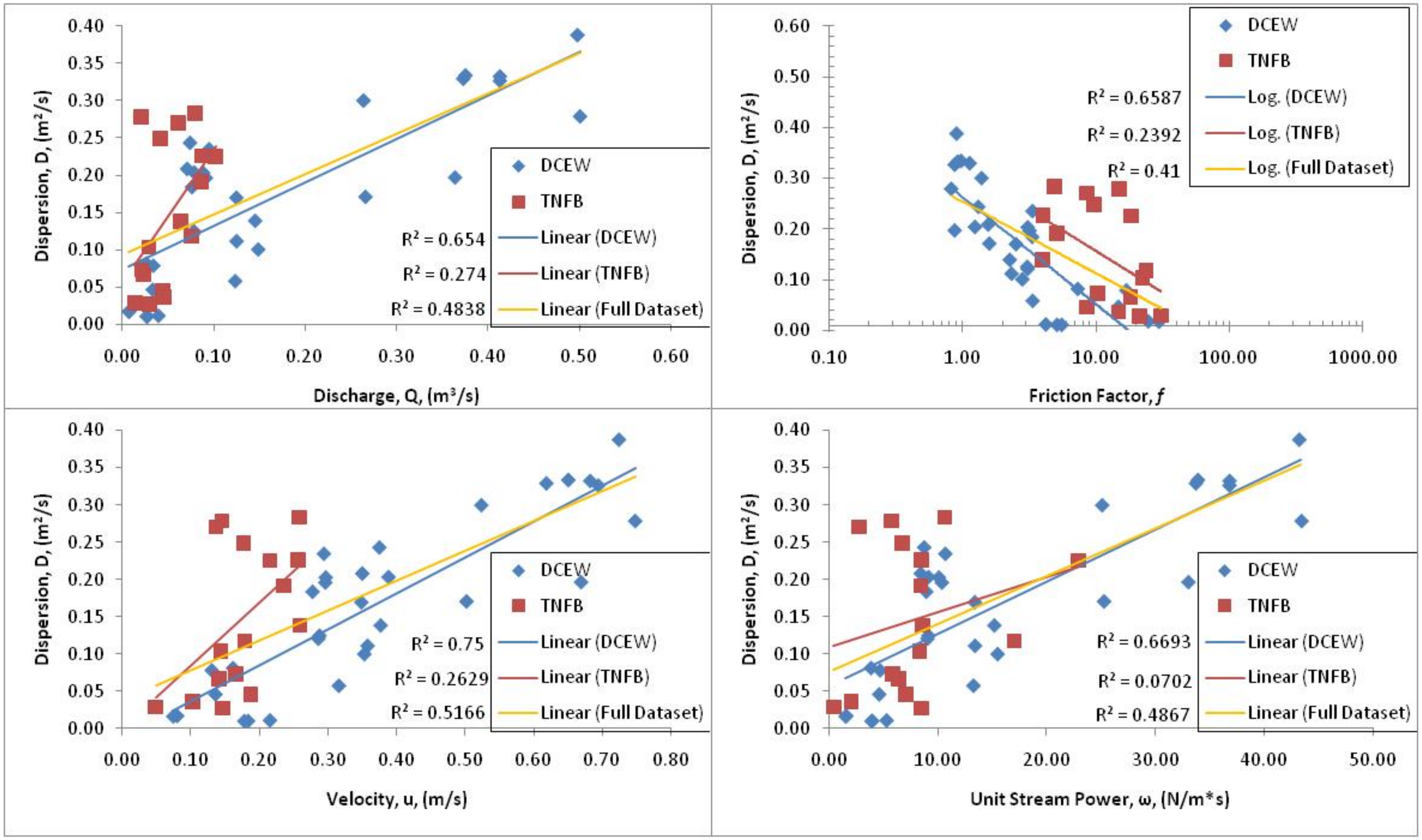

Figure A.1. Dispersion verses discharge, velocity, friction factor, and unit stream power.

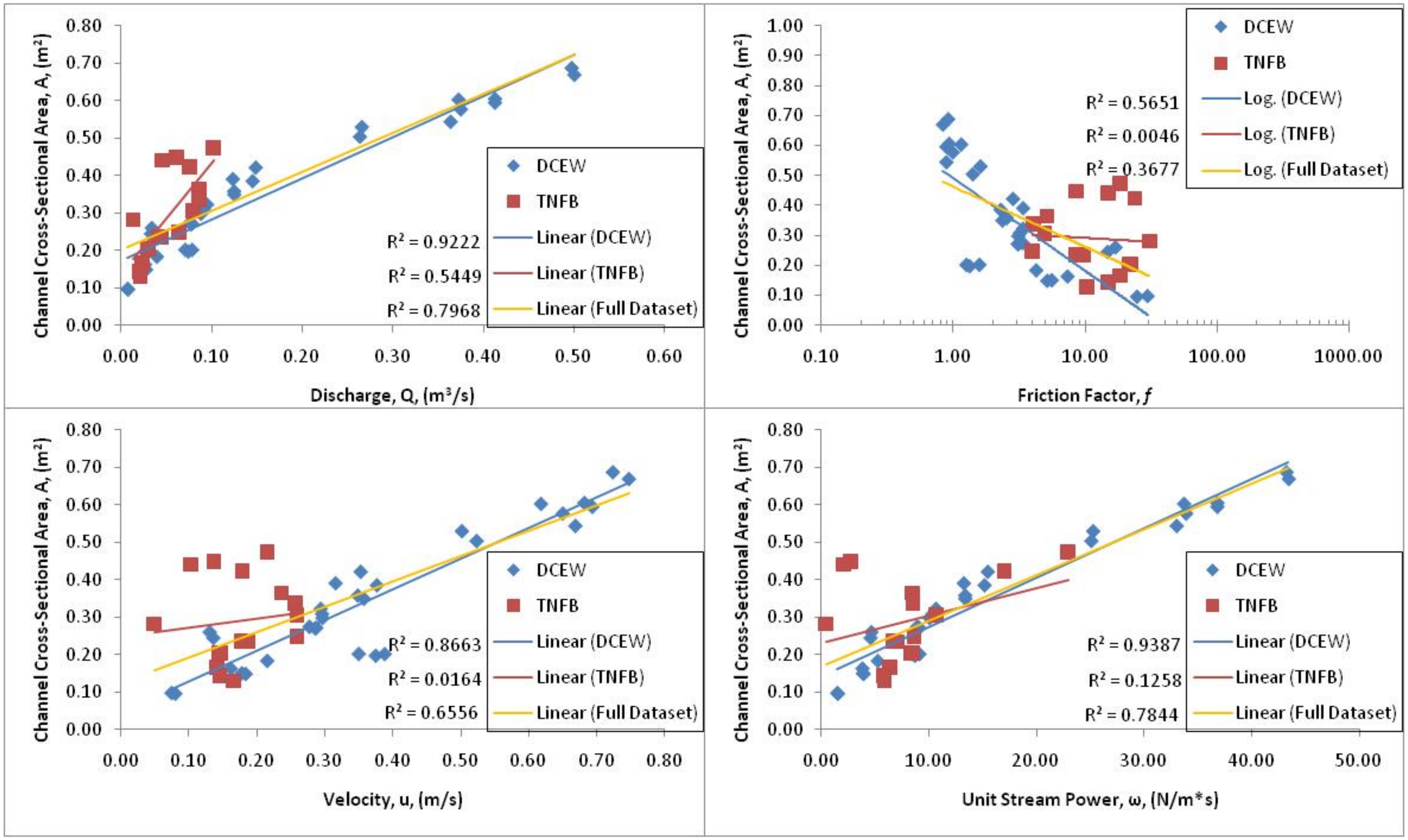

Figure A.2. Channel cross-sectional area verses discharge, velocity, friction factor, and unit stream power.

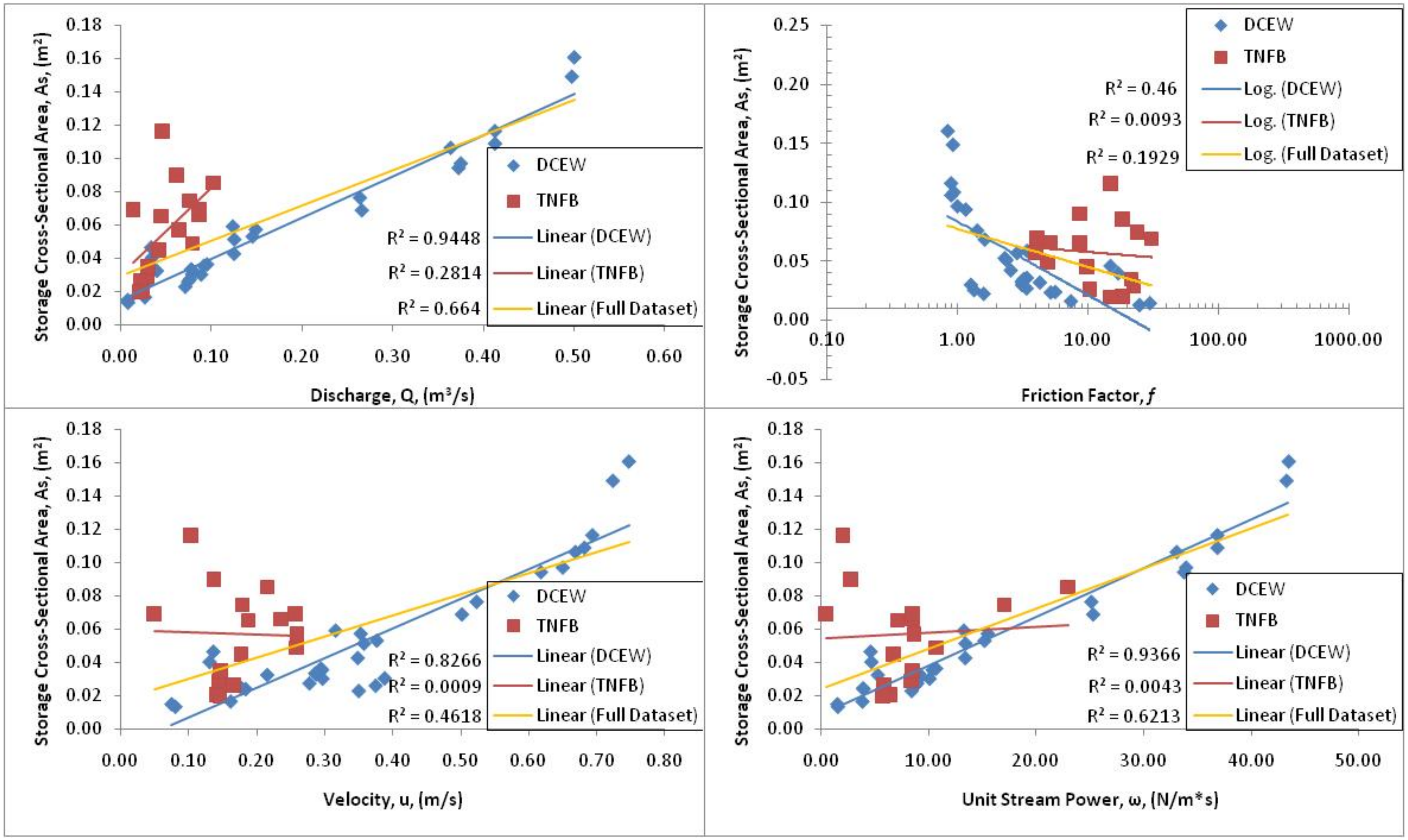

Figure A.3. Storage cross-sectional area verses discharge, velocity, friction factor, and unit stream power.

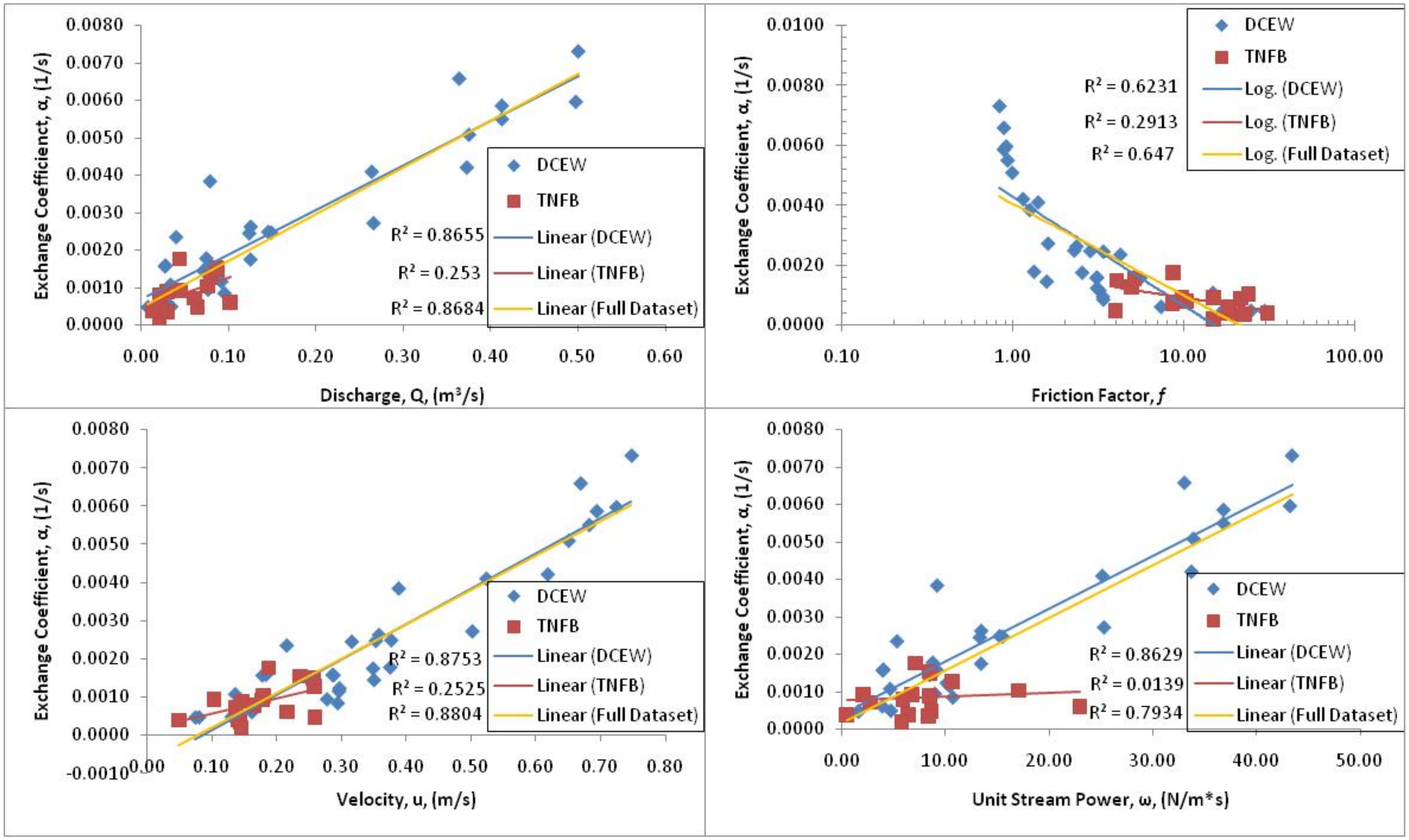

Figure A.4. Exchange coefficient verses discharge, velocity, friction factor, and unit stream power.

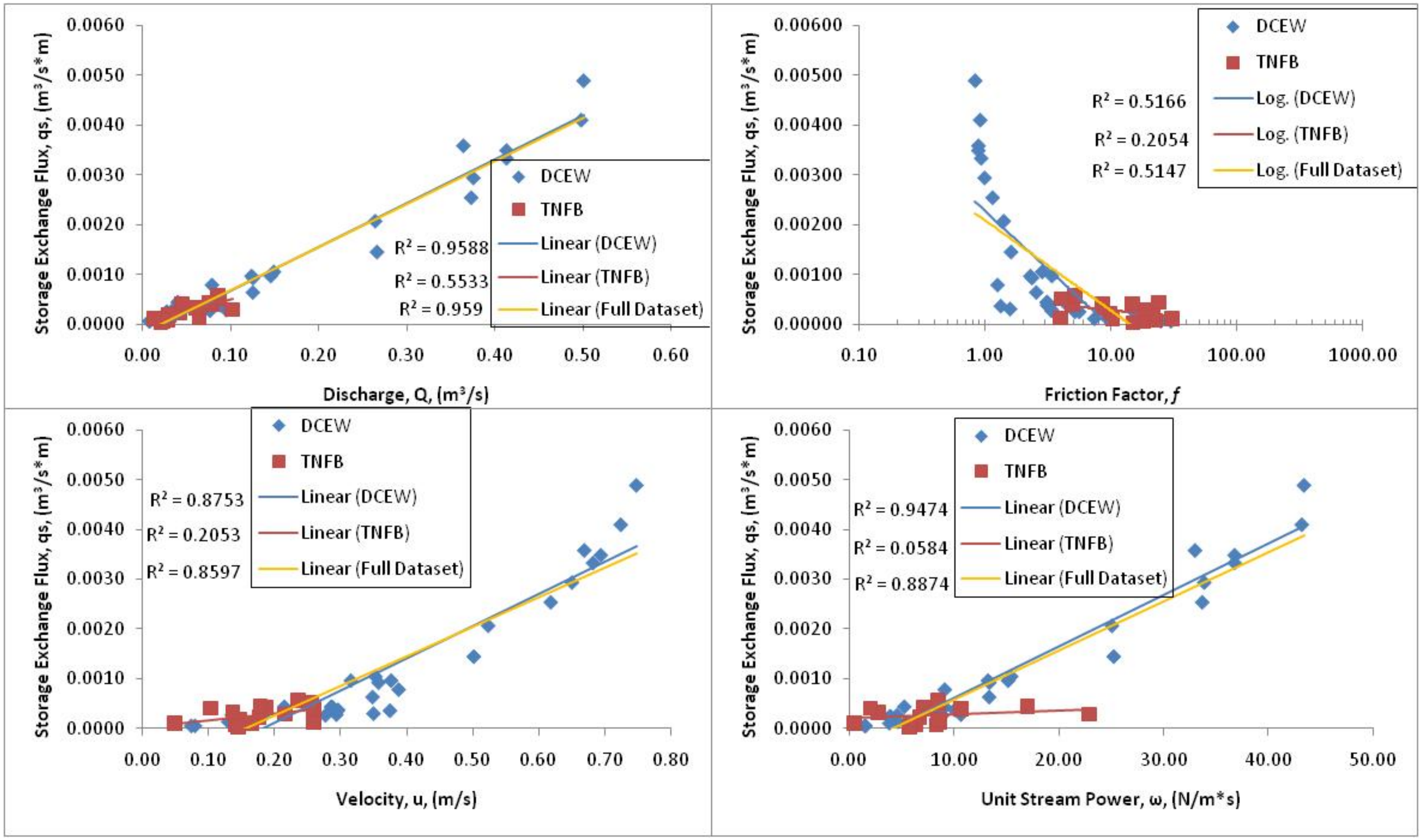

Figure A.5. Storage exchange flux verses discharge, velocity, friction factor, and unit stream power.

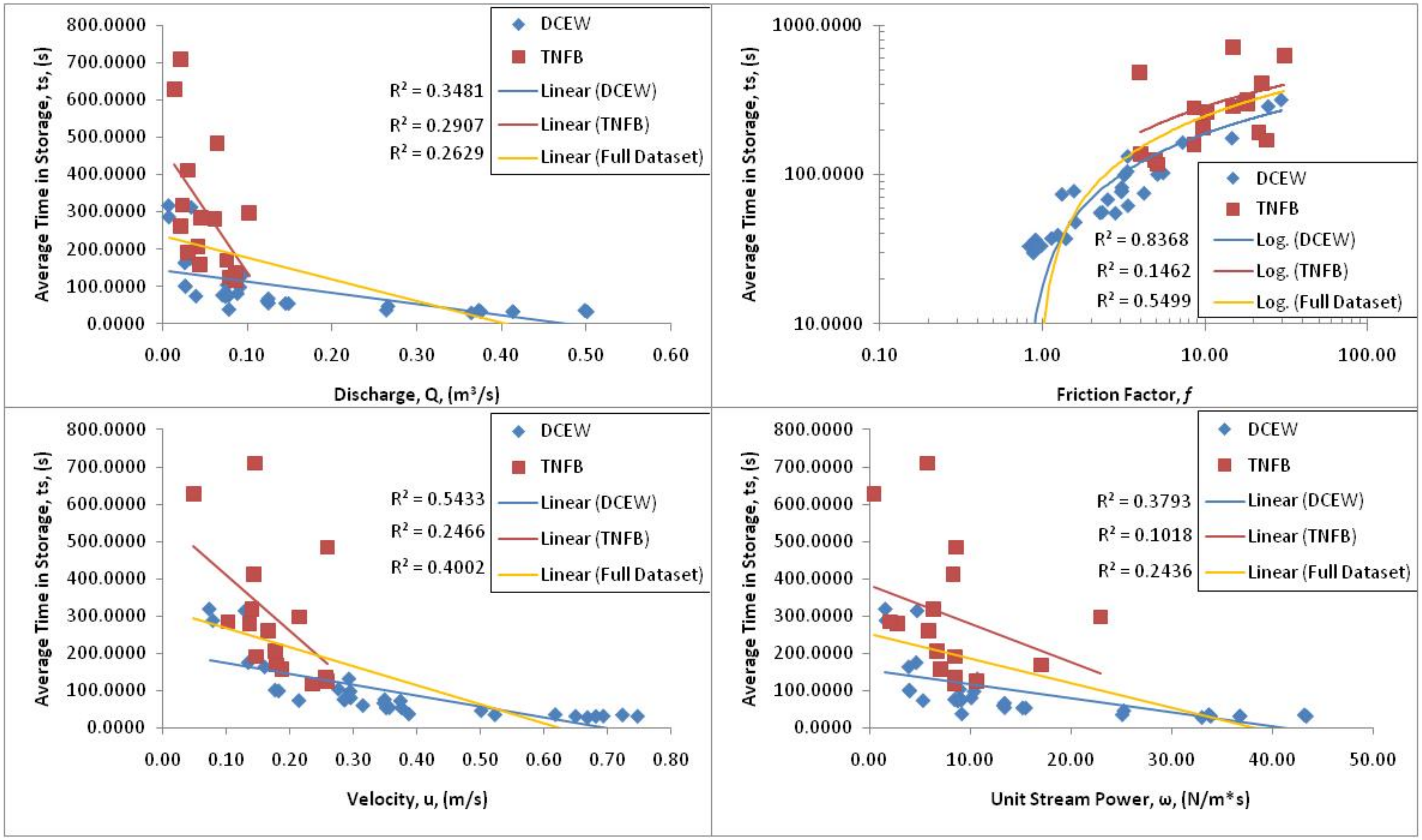

Figure A.6. Average time in storage verses discharge, velocity, friction factor, and unit stream power.

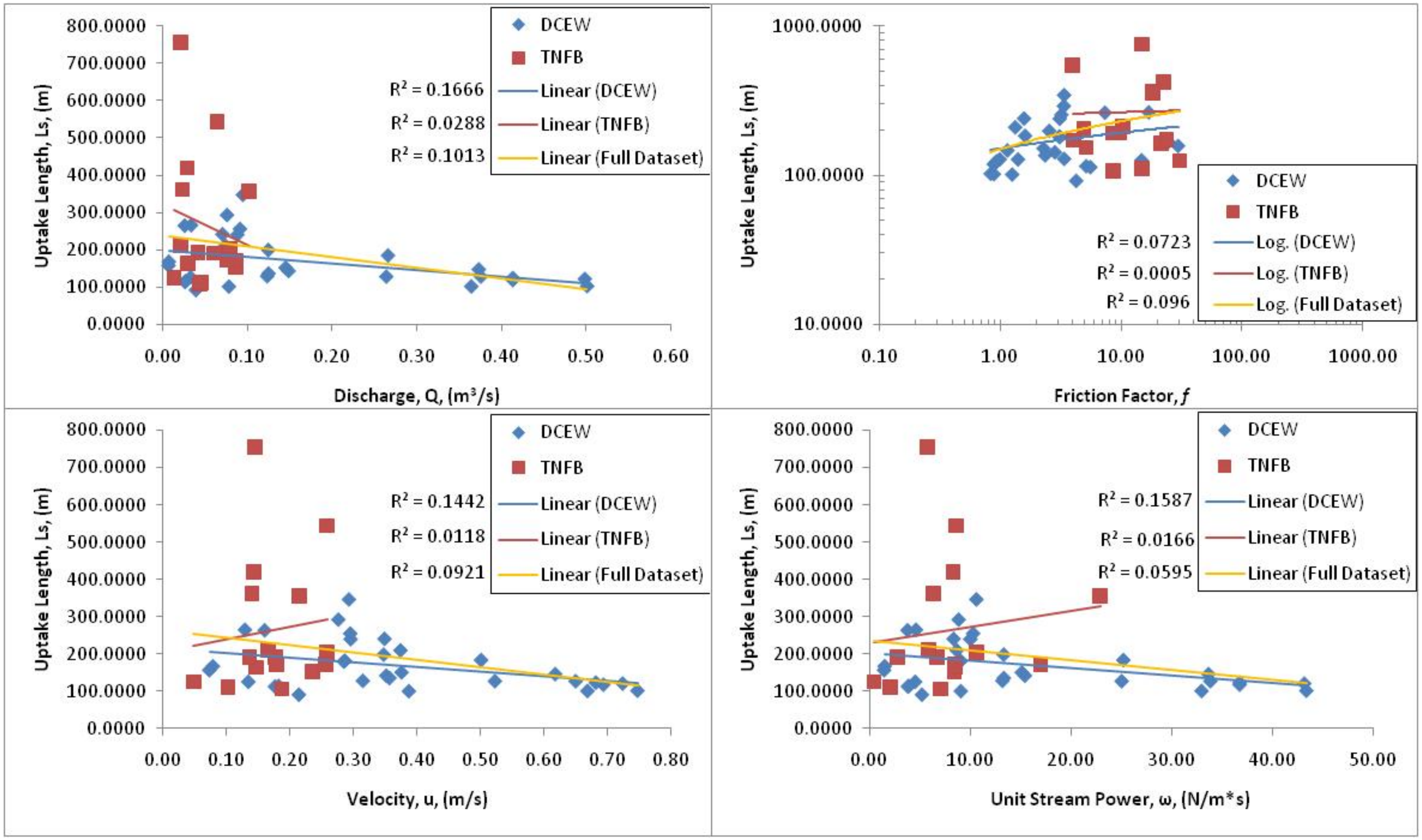

Figure A.7. Uptake length verses discharge, velocity, friction factor, and unit stream power.

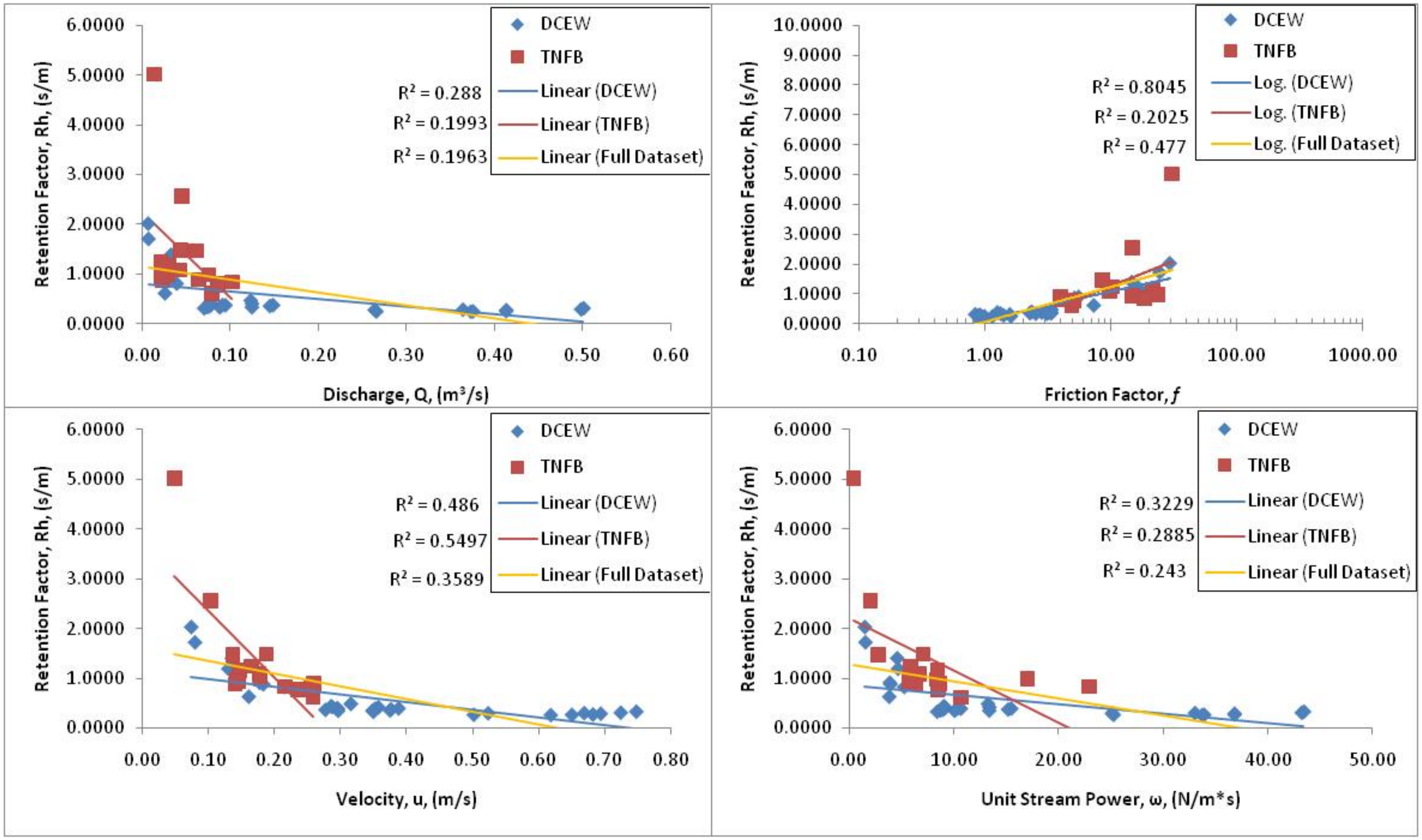

Figure A.8. Retention factor verses discharge, velocity, friction factor, and unit stream power.

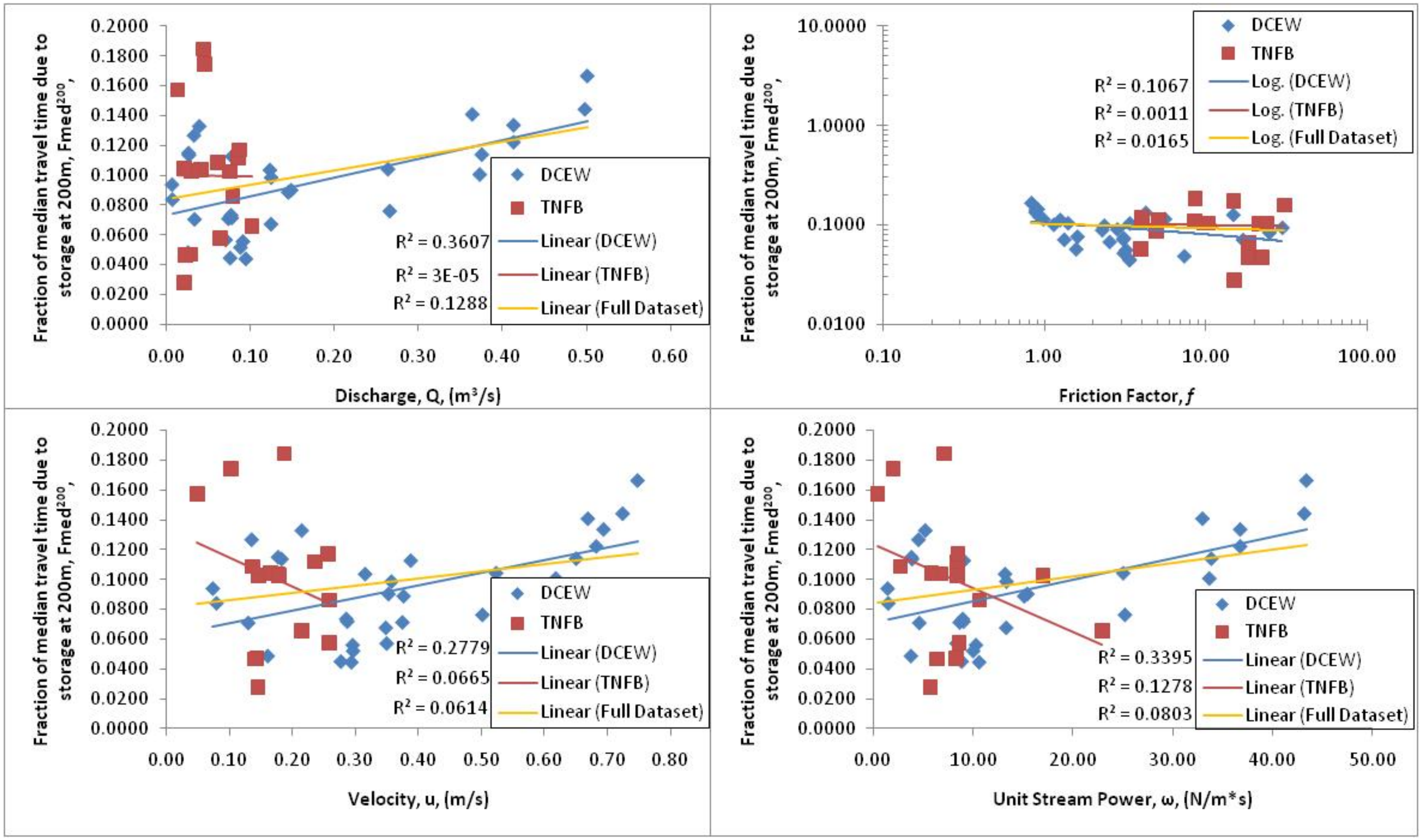

Figure A.9. Fraction of median travel time due to storage at 200m verses discharge, velocity, friction factor, and unit stream power.

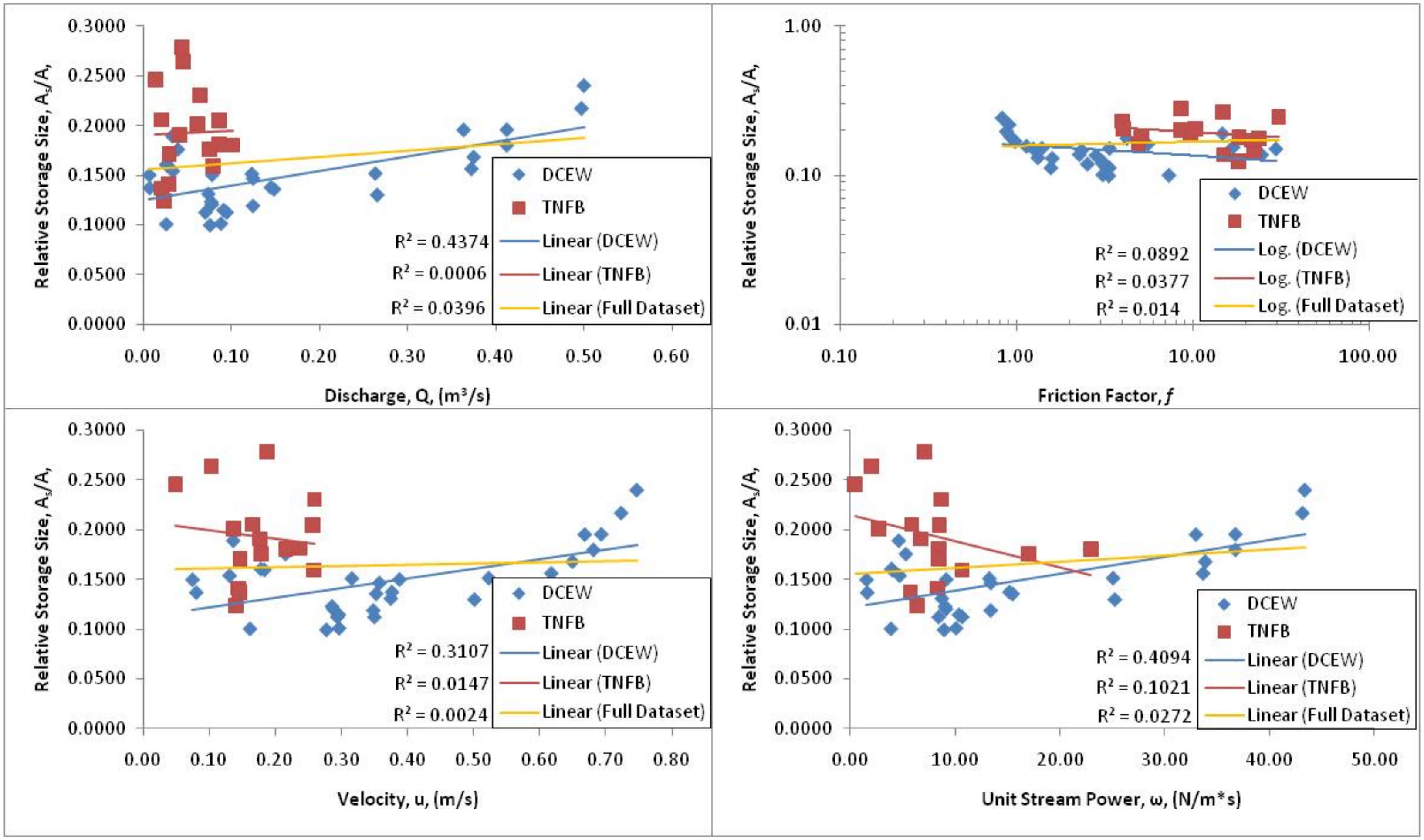

Figure A.10. Relative storage size verses discharge, velocity, friction factor, and unit stream power.

APPENDIX B

Correlation Tables

Table B.1. Correlation Tables for Dry Creek Data

Dry Creek n= 31

	D vs Q	D vs u	D vs f	D vs w
r	0.809	0.866	-0.589	0.818
R^2	0.654	0.750	0.347	0.669
T-value	7.404	9.327	-3.922	7.662
p-value	0.000	0.000	0.000	0.000

	q_s vs Q	q_s vs u	q_s vs f	q_s vs w
r	0.979	0.936	-0.434	0.973
R^2	0.959	0.875	0.188	0.947
T-value	25.977	14.271	-2.592	22.850
p-value	0.000	0.000	0.015	0.000

	A vs Q	A vs u	A vs f	A vs w
r	0.960	0.931	-0.551	0.969
R^2	0.922	0.866	0.304	0.939
T-value	18.537	13.709	-3.556	21.075
p-value	0.000	0.000	0.001	0.000

	t_s vs Q	t_s vs u	t_s vs f	t_s vs w
r	-0.590	-0.737	0.941	-0.616
R^2	0.348	0.543	0.886	0.379
T-value	-3.935	-5.874	15.043	-4.210
p-value	0.000	0.000	0.000	0.000

	A_s vs Q	A_s vs u	A_s vs f	A_s vs w
r	0.972	0.909	-0.428	0.968
R^2	0.945	0.827	0.183	0.937
T-value	22.276	11.757	-2.547	20.692
p-value	0.000	0.000	0.016	0.000

	L_s vs Q	L_s vs u	L_s vs f	L_s vs w
r	-0.408	-0.380	0.100	-0.398
R^2	0.167	0.144	0.010	0.159
T-value	-2.408	-2.210	0.539	-2.339
p-value	0.023	0.035	0.594	0.026

	α vs Q	α vs u	α vs f	α vs w
r	0.930	0.936	-0.522	0.929
R^2	0.866	0.875	0.273	0.863
T-value	13.663	14.270	-3.298	13.508
p-value	0.000	0.000	0.003	0.000

	R_h vs Q	R_h vs u	R_h vs f	R_h vs w
r	-0.537	-0.697	0.964	-0.568
R^2	0.288	0.486	0.929	0.323
T-value	-3.425	-5.236	19.504	-3.719
p-value	0.002	0.000	0.000	0.001

Cont. Table B.1. Correlation Tables for Dry Creek Data.

	A_s/A vs Q	A_s/A vs u	A_s/A vs f	A_s/A vs w
r	0.661	0.557	-0.053	0.640
R^2	0.437	0.311	0.003	0.409
T-value	4.749	3.616	-0.284	4.483
p-value	0.000	0.001	0.779	0.000

	F_{med}^{200} vs Q	F_{med}^{200} vs u	F_{med}^{200} vs f	F_{med}^{200} vs w
r	0.601	0.527	-0.110	0.583
R^2	0.361	0.278	0.012	0.340
T-value	4.045	3.341	-0.596	3.861
p-value	0.000	0.002	0.555	0.001

Table B.2. Correlation Tables for North Fork Boise Tributaries Data

North Fork Boise n= 16

	D vs Q	D vs u	D vs f	D vs w
r	0.523	0.513	-0.515	0.265
R^2	0.274	0.263	0.266	0.070
T-value	2.299	2.235	-2.251	1.028
p-value	0.037	0.042	0.041	0.321

	q_s vs Q	q_s vs u	q_s vs f	q_s vs w
r	0.744	0.453	-0.424	0.242
R^2	0.553	0.205	0.179	0.058
T-value	4.164	1.902	-1.750	0.932
p-value	0.001	0.078	0.102	0.367

	A vs Q	A vs u	A vs f	A vs w
r	0.738	0.128	-0.039	0.355
R^2	0.545	0.016	0.001	0.126
T-value	4.094	0.484	-0.144	1.419
p-value	0.001	0.636	0.887	0.178

	t_s vs Q	t_s vs u	t_s vs f	t_s vs w
r	-0.539	-0.497	0.422	-0.319
R^2	0.291	0.247	0.178	0.102
T-value	-2.396	-2.140	1.744	-1.260
p-value	0.031	0.050	0.103	0.228

	A_s vs Q	A_s vs u	A_s vs f	A_s vs w
r	0.531	-0.029	-0.070	0.066
R^2	0.281	0.001	0.005	0.004
T-value	2.342	-0.110	-0.264	0.246
p-value	0.035	0.914	0.796	0.809

	L_s vs Q	L_s vs u	L_s vs f	L_s vs w
r	-0.170	0.109	-0.005	0.129
R^2	0.029	0.012	0.000	0.017
T-value	-0.644	0.409	-0.019	0.486
p-value	0.530	0.689	0.985	0.634

	α vs Q	α vs u	α vs f	α vs w
r	0.503	0.502	-0.530	0.118
R^2	0.253	0.252	0.281	0.014
T-value	2.178	2.175	-2.340	0.444
p-value	0.047	0.047	0.035	0.664

	R_h vs Q	R_h vs u	R_h vs f	R_h vs w
r	-0.446	-0.741	0.546	-0.537
R^2	0.199	0.550	0.298	0.288
T-value	-1.867	-4.134	2.438	-2.382
p-value	0.083	0.001	0.029	0.032

Cont. Table B.2. Correlation Tables for North Fork Boise Tributaries Data.

	A_s/A vs Q	A_s/A vs u	A_s/A vs f	A_s/A vs w
r	0.024	-0.121	-0.159	-0.320
R^2	0.001	0.015	0.025	0.102
T-value	0.090	-0.457	-0.604	-1.262
p-value	0.929	0.655	0.556	0.228

	F_{med}^{200} vs Q	F_{med}^{200} vs u	F_{med}^{200} vs f	F_{med}^{200} vs w
r	-0.006	-0.258	-0.016	-0.358
R^2	0.000	0.067	0.000	0.128
T-value	-0.022	-0.999	-0.059	-1.432
p-value	0.983	0.335	0.954	0.174

Table B.3. Correlation Tables for Dry Creek and North Fork Boise Tributaries Data.

All Sites n= 47

	D vs Q	D vs u	D vs f	D vs w
r	0.696	0.719	-0.529	0.698
R^2	0.484	0.517	0.280	0.487
T-value	6.494	6.935	-4.187	6.532
p-value	0.000	0.000	0.000	0.000

	A vs Q	A vs u	A vs f	A vs w
r	0.893	0.810	-0.432	0.886
R^2	0.797	0.656	0.187	0.784
T-value	13.284	9.256	-3.215	12.796
p-value	0.000	0.000	0.002	0.000

	A_s vs Q	A_s vs u	A_s vs f	A_s vs w
r	0.815	0.680	-0.263	0.788
R^2	0.664	0.462	0.069	0.621
T-value	9.431	6.214	-1.829	8.592
p-value	0.000	0.000	0.074	0.000

	α vs Q	α vs u	α vs f	α vs w
r	0.932	0.938	-0.581	0.891
R^2	0.868	0.880	0.337	0.793
T-value	17.233	18.198	-4.782	13.146
p-value	0.000	0.000	0.000	0.000

	q_s vs Q	q_s vs u	q_s vs f	q_s vs w
r	0.979	0.927	-0.475	0.942
R^2	0.959	0.860	0.226	0.887
T-value	32.423	16.606	-3.621	18.834
p-value	0.000	0.000	0.001	0.000

	t_s vs Q	t_s vs u	t_s vs f	t_s vs w
r	-0.513	-0.633	0.730	-0.494
R^2	0.263	0.400	0.532	0.244
T-value	-4.007	-5.479	7.157	-3.807
p-value	0.000	0.000	0.000	0.000

	L_s vs Q	L_s vs u	L_s vs f	L_s vs w
r	-0.318	-0.303	0.209	-0.244
R^2	0.101	0.092	0.044	0.060
T-value	-2.253	-2.137	1.431	-1.687
p-value	0.029	0.038	0.159	0.098

	R_h vs Q	R_h vs u	R_h vs f	R_h vs w
r	-0.443	-0.599	0.752	-0.493
R^2	0.196	0.359	0.566	0.243
T-value	-3.316	-5.019	7.656	-3.801
p-value	0.002	0.000	0.000	0.000

Cont. Table B.3. Correlation Tables for Dry Creek and North Fork Boise Tributaries Data.

	A_s/A vs Q	A_s/A vs u	A_s/A vs f	A_s/A vs w
r	0.199	0.049	0.170	0.165
R^2	0.040	0.002	0.029	0.027
T-value	1.363	0.328	1.158	1.121
p-value	0.180	0.745	0.253	0.268

	F_{med}^{200} vs Q	F_{med}^{200} vs u	F_{med}^{200} vs f	F_{med}^{200} vs w
r	0.359	0.248	-0.020	0.283
R^2	0.129	0.061	0.000	0.080
T-value	2.580	1.716	-0.135	1.982
p-value	0.013	0.093	0.893	0.054

APPENDIX C

Data Charts

Table C.1. Dry Creek Hydraulic Parameters Data

Table C.1 Dry Creek Hydraulic Parameters Data												
Stream	DATE	Q (m^3/s)	D (m^2/s)	A (m^2)	A_s (m^2)	α (1/s)	u (m/s)	f	ω (N/m*s)	Slope (m/m)	Width (m)	Dal
Dry Creek	26-Nov-08	0.0333	0.0461	0.2454	0.0464	0.0011	0.1355	14.73	4.59	0.0338	2.40	6.98
Dry Creek	26-Nov-08	0.0340	0.0784	0.2610	0.0402	0.0005	0.1302	16.91	4.67	0.0338	2.41	3.95
Dry Creek	11-Apr-09	0.4979	0.3881	0.6879	0.1492	0.0060	0.7238	0.91	43.21	0.0338	3.82	6.47
Dry Creek	11-Apr-09	0.5007	0.2789	0.6699	0.1608	0.0073	0.7474	0.83	43.42	0.0338	3.82	7.07
Dry Creek	17-Apr-09	0.3641	0.1969	0.5445	0.1064	0.0066	0.6687	0.88	33.01	0.0338	3.66	8.44
Dry Creek	17-Apr-09	0.3729	0.3295	0.6034	0.0942	0.0042	0.6180	1.14	33.70	0.0338	3.67	7.06
Dry Creek	17-Apr-09	0.3754	0.3340	0.5775	0.0970	0.0051	0.6501	0.99	33.89	0.0338	3.67	7.62
Dry Creek	24-Apr-09	0.4131	0.3267	0.5956	0.1165	0.0059	0.6936	0.88	36.79	0.0338	3.72	7.23
Dry Creek	24-Apr-09	0.4131	0.3328	0.6058	0.1089	0.0055	0.6819	0.93	36.79	0.0338	3.72	7.41
Dry Creek	8-May-09	0.2660	0.1709	0.5304	0.0688	0.0027	0.5015	1.60	25.26	0.0338	3.49	6.62
Dry Creek	8-May-09	0.2639	0.3002	0.5044	0.0764	0.0041	0.5232	1.40	25.09	0.0338	3.49	8.33
Dry Creek	20-May-09	0.1488	0.1003	0.4221	0.0572	0.0025	0.3525	2.82	15.48	0.0338	3.19	8.22
Dry Creek	20-May-09	0.1453	0.1387	0.3860	0.0530	0.0025	0.3764	2.27	15.17	0.0338	3.17	7.66
Dry Creek	28-May-09	0.0950	0.2349	0.3233	0.0363	0.0008	0.2937	3.36	10.66	0.0338	2.95	4.00
Dry Creek	28-May-09	0.0915	0.1963	0.3094	0.0354	0.0012	0.2957	3.20	10.35	0.0338	2.93	5.33

Cont. Table C.1 Dry Creek Hydraulic Parameters Data												
Stream	DATE	Q (m^3/s)	D (m^2/s)	A (m^2)	A_s (m^2)	α (1/s)	u (m/s)	f	ω (N/m*s)	Slope (m/m)	Width (m)	DaI
Dry Creek	28-May-09	0.0885	0.2031	0.2987	0.0301	0.0012	0.2963	3.09	10.07	0.0338	2.91	6.36
Dry Creek	3-Jun-09	0.0785	0.2037	0.2024	0.0304	0.0038	0.3879	1.25	9.13	0.0338	2.85	10.63
Dry Creek	3-Jun-09	0.0742	0.2435	0.1980	0.0259	0.0018	0.3747	1.32	8.72	0.0338	2.82	5.75
Dry Creek	3-Jun-09	0.0709	0.2085	0.2027	0.0227	0.0014	0.3497	1.57	8.40	0.0338	2.80	5.76
Dry Creek	18-Jun-09	0.1235	0.0577	0.3914	0.0591	0.0024	0.3156	3.37	13.25	0.0338	3.09	8.28
Dry Creek	18-Jun-09	0.1251	0.1114	0.3501	0.0513	0.0026	0.3574	2.35	13.39	0.0338	3.10	8.05
Dry Creek	18-Jun-09	0.1249	0.1698	0.3586	0.0426	0.0018	0.3483	2.53	13.38	0.0338	3.10	6.63
Dry Creek	24-Jun-09	0.0783	0.1249	0.2725	0.0328	0.0016	0.2872	3.07	9.10	0.0338	2.85	7.15
Dry Creek	24-Jun-09	0.0774	0.1209	0.2712	0.0333	0.0016	0.2856	3.10	9.02	0.0338	2.84	7.09
Dry Creek	24-Jun-09	0.0763	0.1839	0.2752	0.0273	0.0009	0.2771	3.35	8.91	0.0338	2.84	5.30
Dry Creek	1-Jul-09	0.0396	0.0111	0.1842	0.0324	0.0023	0.2150	4.24	5.27	0.0338	2.49	10.24
Dry Creek	15-Jul-09	0.0274	0.0104	0.1493	0.0238	0.0016	0.1831	5.13	3.94	0.0338	2.30	8.83
Dry Creek	15-Jul-09	0.0269	0.0102	0.1513	0.0243	0.0016	0.1775	5.56	3.89	0.0338	2.29	8.93
Dry Creek	15-Jul-09	0.0264	0.0814	0.1638	0.0164	0.0006	0.1612	7.33	3.84	0.0338	2.28	5.82
Dry Creek	27-Aug-09	0.0077	0.0172	0.0966	0.0132	0.0005	0.0797	24.62	1.56	0.0338	1.63	6.93
Dry Creek	27-Aug-09	0.0073	0.0165	0.0985	0.0148	0.0005	0.0741	29.61	1.51	0.0338	1.61	6.82

Table C.2. Dry Creek Hydraulic Metric Data

Table C.2 Dry Creek Hydraulic Metric Data							
Stream	DATE	q_s, (m^3/s*m)	t_s, (s)	L_s, (m)	R_h, (s/m)	F_{med}^{200} (%)	A_s/A
Dry Creek	26-Nov-08	2.64E-04	175.8	126.0	1.3952	12.65	0.1891
Dry Creek	26-Nov-08	1.28E-04	314.0	265.7	1.1819	7.05	0.1539
Dry Creek	11-Apr-09	4.10E-03	36.4	121.3	0.2997	14.40	0.2170
Dry Creek	11-Apr-09	4.90E-03	32.8	102.2	0.3212	16.62	0.2401
Dry Creek	17-Apr-09	3.59E-03	29.7	101.5	0.2921	14.06	0.1953
Dry Creek	17-Apr-09	2.54E-03	37.1	146.8	0.2527	10.05	0.1561
Dry Creek	17-Apr-09	2.94E-03	33.0	127.8	0.2584	11.37	0.1680
Dry Creek	24-Apr-09	3.49E-03	33.4	118.4	0.2820	13.34	0.1956
Dry Creek	24-Apr-09	3.33E-03	32.7	124.0	0.2637	12.20	0.1798
Dry Creek	8-May-09	1.44E-03	47.7	184.3	0.2586	7.60	0.1297
Dry Creek	8-May-09	2.07E-03	37.0	127.8	0.2894	10.40	0.1514
Dry Creek	20-May-09	1.04E-03	54.9	142.7	0.3846	9.00	0.1356
Dry Creek	20-May-09	9.60E-04	55.2	151.4	0.3649	8.85	0.1373
Dry Creek	28-May-09	2.74E-04	132.6	347.1	0.3819	4.42	0.1122
Dry Creek	28-May-09	3.58E-04	98.9	255.6	0.3869	5.57	0.1144
Dry Creek	28-May-09	3.68E-04	81.8	240.3	0.3402	5.17	0.1008
Dry Creek	3-Jun-09	7.77E-04	39.1	101.0	0.3868	11.24	0.1500
Dry Creek	3-Jun-09	3.52E-04	73.5	210.5	0.3491	7.09	0.1308
Dry Creek	3-Jun-09	2.94E-04	77.4	241.4	0.3205	5.68	0.1121
Dry Creek	18-Jun-09	9.59E-04	61.6	128.8	0.4785	10.34	0.1510
Dry Creek	18-Jun-09	9.19E-04	55.8	136.1	0.4099	9.84	0.1465
Dry Creek	18-Jun-09	6.28E-04	67.9	199.0	0.3411	6.73	0.1188

Cont. Table C.2 Dry Creek Hydraulic Metric Data

Stream	DATE	q_s, ($m^3/s*m$)	t_s, (s)	L_s, (m)	R_h, (s/m)	F_{med}^{200} (%)	A_s/A
Dry Creek	24-Jun-09	4.29E-04	76.4	182.4	0.4187	7.15	0.1203
Dry Creek	24-Jun-09	4.29E-04	77.6	180.5	0.4300	7.33	0.1228
Dry Creek	24-Jun-09	2.60E-04	104.9	292.9	0.3580	4.47	0.0992
Dry Creek	1-Jul-09	4.33E-04	74.8	91.5	0.8171	13.26	0.1757
Dry Creek	15-Jul-09	2.38E-04	100.3	115.1	0.8718	11.35	0.1597
Dry Creek	15-Jul-09	2.37E-04	102.5	113.3	0.9050	11.47	0.1606
Dry Creek	15-Jul-09	9.99E-05	164.3	264.2	0.6220	4.84	0.1002
Dry Creek	27-Aug-09	4.59E-05	287.9	167.9	1.7149	8.37	0.1367
Dry Creek	27-Aug-09	4.63E-05	318.5	157.5	2.0218	9.37	0.1498

Table C.3. Tributaries of the North Fork of the Boise Hydraulic Parameter Data

Table C.3 Tributaries of the North Fork of the Boise Hydraulic Parameter Data												
Stream	Date	Q (m^3/s)	D (m^2/s)	A (m^2)	A_s (m^2)	α (1/s)	u (m/s)	f	ω (N/m*s)	Slope (m/m)	Width (m)	DaI
Big Owl 2	21-Sep-08	0.0440	0.0453	0.2346	0.0654	0.0018	0.1876	8.6	7.1	0.0396	2.41	5.38
Big Owl 2	21-Sep-08	0.0418	0.2486	0.2364	0.0451	0.0009	0.1769	9.7	6.7	0.0396	2.41	4.07
Hunter 1	20-Sep-08	0.0793	0.2831	0.3065	0.0489	0.0013	0.2588	4.91	10.65	0.0320	2.34	4.47
Hunter 2	20-Sep-08	0.0643	0.1384	0.2482	0.0572	0.0005	0.2591	3.97	8.64	0.0320	2.34	1.23
German 1	14-Sep-08	0.0860	0.1913	0.3645	0.0660	0.0015	0.2360	5.13	8.44	0.0394	3.94	5.34
German 2	14-Sep-08	0.0867	0.2260	0.3380	0.0692	0.0015	0.2564	4.03	8.51	0.0394	3.94	4.28
Hungarian 1	13-Sep-08	0.0294	0.1035	0.2041	0.0288	0.0003	0.1438	22.38	8.33	0.0632	2.18	2.41
Hungarian 2	13-Sep-08	0.0298	0.0274	0.2033	0.0347	0.0009	0.1468	21.39	8.47	0.0632	2.18	3.13
Beaver 1	19-Sep-08	0.0233	0.0665	0.1654	0.0205	0.0004	0.1408	18.25	6.38	0.0480	1.72	5.65
Beaver 2	19-Sep-08	0.0214	0.0731	0.1291	0.0265	0.0008	0.1656	10.31	5.86	0.0480	1.72	5.57
Beaver 2	19-Sep-08	0.0210	0.2784	0.1443	0.0197	0.0002	0.1456	14.91	5.75	0.0480	1.72	2.20
Trail 1	20-Sep-08	0.0758	0.1177	0.4240	0.0744	0.0010	0.1788	23.83	17.03	0.0576	2.51	4.85
Trail 2	20-Sep-08	0.1021	0.2251	0.4739	0.0854	0.0006	0.2154	18.34	22.94	0.0576	2.51	2.30
L. Beaver 1	6-Sep-08	0.0138	0.0290	0.2814	0.0691	0.0004	0.0490	30.65	0.45	0.0073	2.20	5.67
Banner 1	5-Sep-08	0.0614	0.2705	0.4480	0.0901	0.0007	0.1370	8.55	2.75	0.0106	2.32	4.38
Banner 2	1-Sep-08	0.0454	0.0363	0.4402	0.1162	0.0009	0.1031	14.84	2.03	0.0106	2.32	5.38

Table C.4. Tributaries of the North Fork of the Boise Hydraulic Metric Data

Table C.4 Tributaries of the North Fork of the Boise Hydraulic Metric Data							
Stream	Date	q_s, (m^3/s*m)	t_s, (s)	L_s, (m)	R_h, (s/m)	F_{med}^{200} (%)	A_s/A
Big Owl 2	21-Sep-08	4.12E-04	158.4	106.7	1.4846	18.44	0.2785
Big Owl 2	21-Sep-08	2.18E-04	206.7	191.7	1.0782	10.37	0.1907
Hunter 1	20-Sep-08	3.90E-04	125.4	203.4	0.6163	8.61	0.1595
Hunter 2	20-Sep-08	1.18E-04	484.4	544.3	0.8899	5.76	0.2306
German 1	14-Sep-08	5.63E-04	117.2	152.8	0.7673	11.19	0.1811
German 2	14-Sep-08	5.05E-04	137.1	171.6	0.7988	11.70	0.2048
Hungarian 1	13-Sep-08	7.00E-05	411.2	419.1	0.9811	4.69	0.1411
Hungarian 2	13-Sep-08	1.82E-04	191.1	164.2	1.1642	10.28	0.1709
Beaver 1	19-Sep-08	6.44E-05	317.7	361.8	0.8781	4.67	0.1237
Beaver 2	19-Sep-08	1.01E-04	261.4	210.7	1.2403	10.44	0.2054
Beaver 2	19-Sep-08	2.78E-05	709.3	755.0	0.9395	2.80	0.1367
Trail 1	20-Sep-08	4.39E-04	169.5	172.6	0.9822	10.25	0.1756
Trail 2	20-Sep-08	2.87E-04	297.4	355.7	0.8362	6.57	0.1802
L. Beaver 1	6-Sep-08	1.10E-04	627.9	125.2	5.0154	15.73	0.2456
Banner 1	5-Sep-08	3.21E-04	280.4	191.0	1.4680	10.87	0.2011
Banner 2	1-Sep-08	4.08E-04	284.7	111.3	2.5593	17.42	0.2639

Table C.5. Cottonwood Creek Hydraulic Parameter Data

Table C.5 Cottonwood Creek Hydraulic Parameter Data							
Stream	DATE	Q (m^3/s)	D (m^2/s)	A (m^2)	A_s (m^2)	α (1/s)	DaI
Cottonwood	30-Apr-09	0.0680	0.3810	0.0657	0.0074	0.0045	7.33
Cottonwood	30-Apr-09	0.0680	0.5143	0.0679	0.0068	0.0030	5.73

Table C.6. Cottonwood Creek Hydraulic Metric Data

Table C.6 Cottonwood Creek Hydraulic Metric Data							
Stream	DATE	q_s, ($m^3/s*m$)	t_s, (s)	L_s, (m)	R_h, (s/m)	F_{med}^{200} (%)	A_s/A
Cottonwood	30-Apr-09	2.93E-04	25.4	232.2	0.1093	5.87	0.1131
Cottonwood	30-Apr-09	2.07E-04	33.2	329.1	0.1007	4.18	0.1009